© 2014. Published by The Company of Biologists Ltd | Development (2014) 141, 1250-1259 doi:10.1242/dev.103473

RESEARCH ARTICLE

Tryptophan-dependent auxin biosynthesis is required for HD-ZIP III-mediated xylem patterning

Robertas Ursache[1], Shunsuke Miyashima[1], Qingguo Chen[2], Anne Vatén[3], Keiji Nakajima[4], Annelie Carlsbecker[5], Yunde Zhao[2,*], Ykä Helariutta[1,*] and Jan Dettmer[6,*]

ABSTRACT

The development and growth of higher plants is highly dependent on the conduction of water and minerals throughout the plant by xylem vessels. In *Arabidopsis* roots the xylem is organized as an axis of cell files with two distinct cell fates: the central metaxylem and the peripheral protoxylem. During vascular development, high and low expression levels of the class III HD-ZIP transcription factors promote metaxylem and protoxylem identities, respectively. Protoxylem specification is determined by both mobile, ground tissue-emanating miRNA165/6 species, which downregulate, and auxin concentrated by polar transport, which promotes HD-ZIP III expression. However, the factors promoting high *HD-ZIP III* expression for metaxylem identity have remained elusive. We show here that auxin biosynthesis promotes *HD-ZIP III* expression and metaxylem specification. Several auxin biosynthesis genes are expressed in the outer layers surrounding the vascular tissue in *Arabidopsis* root and downregulation of *HD-ZIP III* expression accompanied by specific defects in metaxylem development is seen in auxin biosynthesis mutants, such as *trp2-12*, *wei8 tar2* or a quintuple *yucca* mutant, and in plants treated with L-kynurenine, a pharmacological inhibitor of auxin biosynthesis. Some of the patterning defects can be suppressed by synthetically elevated *HD-ZIP III* expression. Taken together, our results indicate that polar auxin transport, which was earlier shown to be required for protoxylem formation, is not sufficient to establish a proper xylem axis but that root-based auxin biosynthesis is additionally required.

KEY WORDS: *Arabidopsis thaliana*, Auxin biosynthesis, Metaxylem, HD-ZIP III

INTRODUCTION

The plant vascular system, which connects all plant organs, is composed of two conducting tissue types, xylem and phloem. Phloem conducts the photoassimilates produced in the shoot to all other parts of the plant, and xylem functions in the conduction of water and minerals taken up by the roots, and provides structural support. In the *Arabidopsis* root, xylem is organized as a central axis consisting of protoxylem (PX) with spiral secondary cell walls at the marginal positions and metaxylem (MX) with pitted walls at the central position (Fig. 1A,C).

We have previously shown that the class III HD-ZIP genes, *PHABULOSA* (*PHB*), *INTERFASCICULAR FIBERLESS1/REVOLUTA* (*IFL/REV*), *PHAVOLUTA* (*PHV*), *CORONA* (*CNA/AtHB15*) and *AtHB8*, act in a redundant and dosage-dependent manner to control PX and MX patterning and that their expression along the xylem axis is regulated by the mobile microRNA165/6 species emanating from the ground tissue. High and low levels of *HD-ZIP III* confer MX and PX specification, respectively, whereas no *HD-ZIP III* gene expression results in the lack of xylem formation (Carlsbecker et al., 2010; Miyashima et al., 2011).

Besides miRNAs, auxin transport and signaling have been associated with the regulation of HD-ZIP III genes. It is well established that spatiotemporal accumulation of auxin regulates various developmental processes (Sauer et al., 2013; Vanneste and Friml, 2009). Both genetic and pharmacological approaches revealed that auxin concentration maxima (or minima) are established and maintained by polar auxin transport (PAT) employing specific transporters such as PIN, AUX/LAX and PGP proteins (Benková et al., 2003; Cho et al., 2007; Friml et al., 2002; Friml et al., 2004; Friml et al., 2003; Gälweiler et al., 1998; Geisler et al., 2005; Grieneisen et al., 2007; Petrásek et al., 2006; Sorefan et al., 2009; Swarup et al., 2008; Weijers and Jürgens, 2005) and local auxin biosynthesis (Cheng et al., 2006; Cheng et al., 2007; Ikeda et al., 2009; Ljung et al., 2005; Petersson et al., 2009; Stepanova et al., 2008; Tao et al., 2008; Zhao, 2010).

Recently, we provided evidence that certain PIN auxin efflux carriers in procambial cells adjacent to the xylem axis transport auxin towards the PX position and that an auxin maximum at this position is required for protoxylem formation (Bishopp et al., 2011; Mähönen et al., 2006).

Previously, it has been demonstrated that HD-ZIP III gene expression patterns overlap with the pattern of auxin distribution (Izhaki and Bowman, 2007). One of the auxin targets at the PX is the *ATHB8* gene (Bishopp et al., 2011). Lowering auxin levels at the PX by interfering with PAT also lowered AtHB8 expression at this position (Bishopp et al., 2011). In vascular cell specification in leaves, *AtHB8* is co-expressed with *MONOPTEROS/ARF5* (*MP*), a member of the *Arabidopsis* AUXIN RESPONSE FACTOR family, and *PIN1* and functions as a positive regulator of procambial cell proliferation and xylem differentiation (Baima et al., 1995; Baima et al., 2001; Mattsson et al., 2003; Scarpella et al., 2006; Schuetz et al., 2013; Wenzel et al., 2007). A regulatory element in the promoter sequence of *AtHB8* has been found to be directly bound by MP, which thereby regulates auxin-responsive *AtHB8* expression (Donner et al., 2009).

In contrast to PX specification, impaired polar auxin transport has little impact on MX specification (Bishopp et al., 2011). In order to identify the factors promoting MX specification, we characterized

[1]Institute of Biotechnology, Department of Bio and Environmental Sciences, University of Helsinki, FIN-00014, Finland. [2]Section of Cell and Developmental Biology, the University of California San Diego, La Jolla, CA 92093-0116, USA. [3]Department of Biology, Stanford University, Stanford, CA 94305-5020, USA. [4]Graduate School of Biological Sciences, Nara Institute of Science and Technology, 8916-5 Takayama, Ikoma, 630-0192 Nara, Japan. [5]Department of Organismal Biology, Physiological Botany, Uppsala University, and Linnean Center for Plant Biology, Ullsv. 24E, SE-756 51 Uppsala, Sweden. [6]Cell Biology Division, Department of Biology, University of Erlangen-Nuremberg, 91058 Erlangen, Germany.

*Authors for correspondence (yundezhao@ucsd.edu; yrjo.helariutta@helsinki.fi; jan.dettmer@fau.de)

Received 6 September 2013; Accepted 6 January 2014

Development (2014) doi:10.1242/dev.103473

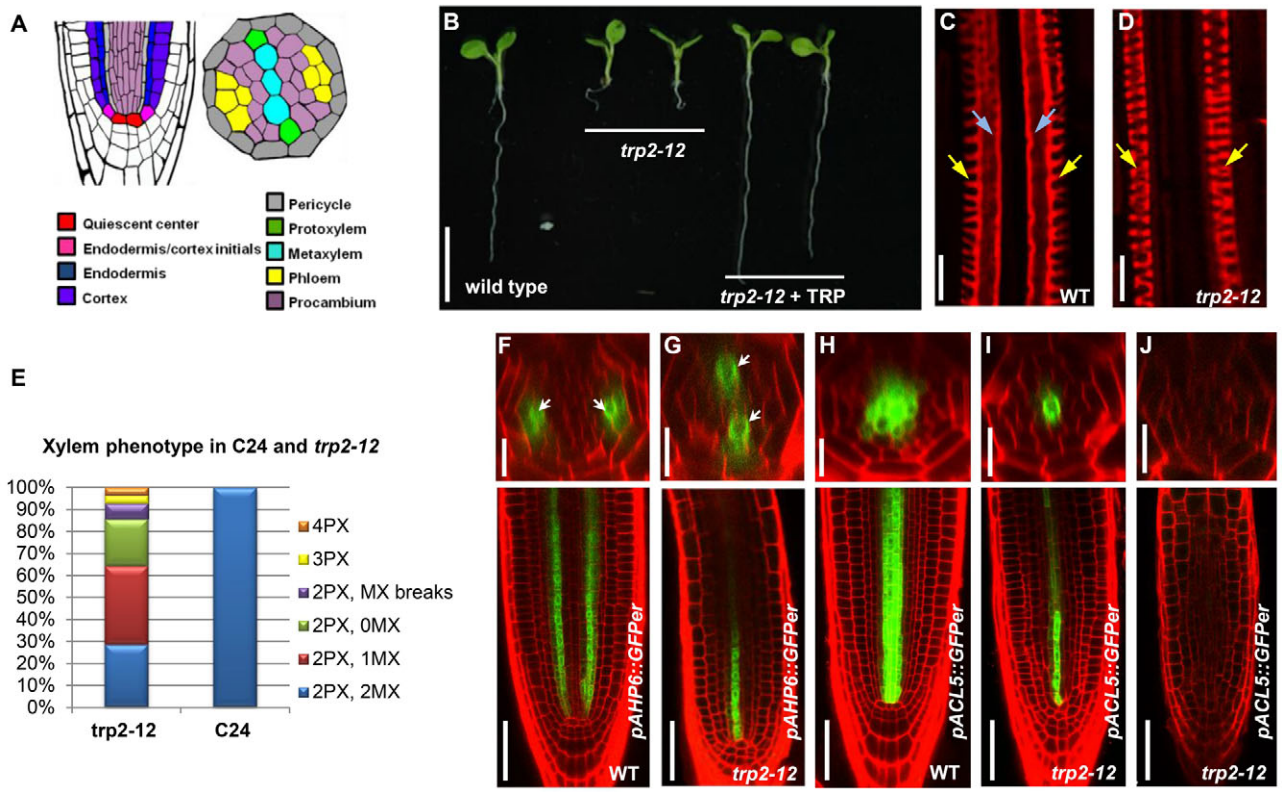

Fig. 1. Xylem phenotype in the *trp2-12* mutant. (A) Schematic of the *Arabidopsis* root. (B) Seedling phenotype of 5-day-old wild type (C24) and *trp2-12* mutants grown on MS medium with and without L-Trp. Scale bar: 0.5 cm. (C,D) Basic-fuchsin-stained xylem of 5-day-old wild-type and *trp2-12* roots. Yellow arrows indicate protoxylem; blue arrows indicate metaxylem. Scale bars: 25 µm. (E) Characterization of the xylem phenotype in 5-day-old wild-type (*n*=28) and *trp2-12* (*n*=28) roots. MX, metaxylem; PX, protoxylem. (F,G) *pAHP6::GFPer* in wild-type and *trp2-12* roots, respectively. Scale bars: 50 µm. White arrows indicate *pAHP6::GFPer* signal in protoxylem. (H-J) *pACL5::GFPer* expression in 5-day-old wild-type and *trp2-12* roots. Scale bars: 50 µm for longitudinal and 10 µm for cross sections.

two allelic loss-of-function mutants with dramatically impaired MX development but relatively normal PX formation. Characterization of these mutants, which we isolated from a forward genetic screen, revealed the involvement of auxin biosynthesis in MX specification.

Auxin is primarily produced through tryptophan (Trp)-dependent biosynthesis pathways but a Trp-independent auxin biosynthesis pathway has been also postulated (Chandler, 2009; Cohen et al., 2003; Korasick et al., 2013; Normanly et al., 1993; Ostin et al., 1999; Strader and Bartel, 2008; Woodward and Bartel, 2005; Zhao, 2010). Three gene families are involved in catalyzing specific Trp-dependent auxin biosynthesis steps, the *TRYPTOPHAN AMINOTRANSFERASE OF ARABIDOPSIS1*/*TRYPTOPHAN AMINOTRANSFERASE-RELATED* (*TAA1/TAR;* also known as *CKRC1* and *TAR1*, respectively – TAIR) and *YUCCA* (*YUC*), which have recently been shown to function in the same pathway (Mashiguchi et al., 2011; Stepanova et al., 2011; Won et al., 2011; Zhao, 2012) and *CYTOCHROME P450 79B2/B3* (*CYP79B2/B3*), which define a distinct pathway (Sugawara et al., 2009; Zhao et al., 2002). The auxin precursor Trp is synthesized from chorismate through several catalytic steps (Radwanski and Last, 1995). The final step, the conversion of indole-3-glycerol phosphate to Trp, is catalyzed by an enzyme complex consisting of TRYPTOPHAN SYNTHASE α- and β-subunits (Barczak et al., 1995; Last et al., 1991). In *Arabidopsis*, two homologous genes encode α-subunits and four genes encode β-subunits (*TSB1*, *TSB2*, *TSB3* and *TSBt2*) (Yin et al., 2010; Zhang et al., 2008).

We show that the TSB1-mediated tryptophan biosynthesis and the auxin biosynthesis genes *TAR1*, *TAR2* and *YUCCA3*, *5*, *7*, *8* and *9* are required for high *HD-ZIP III* expression and MX differentiation in the vascular cylinder of the *Arabidopsis thaliana* primary root. Interestingly, PX differentiation is hardly affected by impaired auxin biosynthesis, whereas inhibition of PAT results in loss of PX but normal MX formation. This suggests that root-based auxin biosynthesis and PAT have to be spatially coordinated during xylem development in *Arabidopsis*.

RESULTS

Isolation of mutants with reduced *HD-ZIP III* expression and defects in metaxylem development

In wild-type *Arabidopsis* plants, GFP expressed under the control of the companion-cell-specific *SUCROSE TRANSPORTER2* promoter (*pSUC2*) moves into the sieve elements and is unloaded symplastically into the root tip (Stadler et al., 2005). To identify novel genes involved in vascular development, a forward genetic screen was performed and several mutant seedlings that failed to unload GFP into the root tip were isolated (supplementary material Fig. S1B,C). Two of the identified mutants, *trp2-12* and *trp2-13*, exhibited similarly severe overall phenotypes, including small leaves with dark veins and short agravitropic primary roots (Fig. 1B). Additionally the mutants showed altered cellular organization around the quiescent center (QC; supplementary material Fig. S1E,F). An allelism test revealed that the two mutants were allelic (Fig. 3B).

We next analyzed the status of vascular tissue differentiation in *trp2-12* roots. Examination of mutant root cross sections and the fuchsin-stained xylem axis revealed not only an altered organization of the phloem poles (supplementary material Fig. S1G,H) but also an interesting xylem patterning defect (Fig. 1C-E). Wild-type roots

Development (2014) doi:10.1242/dev.103473

develop a xylem axis consisting of two metaxylem (MX) files flanked by two protoxylem (PX) poles (21/21; Fig. 1C,E). By contrast, in *trp2-12* roots xylem cells with the morphological characteristics of PX were formed and MX formation was severely impaired (20/28; Fig. 1D,E). These mutants either lack MX (Fig. 1D), or form discontinuous MX strands or only one strand. We also observed ectopic PX formation in the MX position in some *trp2-12* roots (Fig. 1E). Consistent with this observation, the expression of the PX marker *pAHP6::GFPer* appears to be unaffected in *trp2-12* roots (Fig. 1F,G), whereas the expression levels of the MX/procambium marker *pACAULIS5 (pACL5)::GFPer* (Muñiz et al., 2008) is severely reduced or absent (Fig. 1H-J).

Because the HD-ZIP III genes play a crucial role in xylem specification, we next assessed whether their expression levels are altered in the *trp2-12* mutant. We performed a qRT-PCR assay and discovered reduced transcript levels of *PHB*, *AtHB8*, *AtHB15* and *PHV*, whereas *REV* expression was slightly elevated in 5-day-old *trp2-12* mutant root tips in comparison with wild-type roots (Fig. 2H). In addition, downregulation of some of the HD-ZIP III genes, including *PHB*, *AtHB8* and *AtHB15*, was confirmed by RNA *in situ* hybridization (Fig. 2E-G) and by examining the reporter constructs *pAtHB8::GFPer* (supplementary material Fig. S2D,E) and *pPHB::PHB:GFP* (Fig. 2A,B). Taken together, our expression analyses all indicate that the expression of most of the HD-ZIPIII genes is downregulated in the *trp2-12* mutant.

Tryptophan biosynthesis is required for *HD-ZIP III* gene expression and vascular patterning

Next we set out to identify the mutant locus using a PCR-based positional cloning approach. Rough mapping revealed that the locus was located between the markers N5-22116697 and N5-22414573 on chromosome 5 within an approximate 300 kb window. Subsequent sequencing of candidate genes identified point mutations for both alleles in the *At5g54810* locus, which encodes the TRYPTOPHAN SYNTHASE BETA-SUBUNIT 1 (TSB1/TRP2). The mutant alleles were mis-sense mutations causing the following amino acid changes: A315V (*trp2-12*) and G310D (*trp2-13*) (Fig. 3A). In order to verify that the phenotype is indeed caused by the mapped mutations we crossed *trp2-12* and *trp2-13* (expressing *pSUC2::GFP*) with the earlier described *trp2-8* allele (Barczak et al., 1995). Analysis of the F1 progenies revealed that the mutants are allelic (Fig. 3B). Additionally we were able to complement *trp2-12* (and *trp2-13*) with a 5080 bp genomic DNA encompassing the gene (1930 bp) and the upstream region (3150 bp). We subsequently made a translational and transcriptional fusion to investigate *TSB1* expression during root development. The translational *pTSB1::TSB1-YFP* was able to complement the *trp2-12* phenotype (Fig. 3B). The fusion protein was observed in plastids, as predicted *in silico* (supplementary material Fig. S1O-Q). Introduction of the transcriptional *pTSB1::GFP/GUS* fusion construct to the wild type revealed that *TSB1* is highly expressed in the root meristem, especially in the early ground tissue and lateral root cap (Fig. 3I).

It has been previously shown that tryptophan synthase mutants can be rescued by externally supplied L-tryptophan (L-Trp) (Jing et al., 2009; Last et al., 1991; Last and Fink, 1988; Müller and Weiler, 2000). We therefore examined *trp2-12* mutants grown on medium supplied with 10 µM L-Trp and found that the mutant phenotypes, including phloem unloading and xylem patterning defects, were completely rescued (supplementary material Fig. S1I-K). Consistent

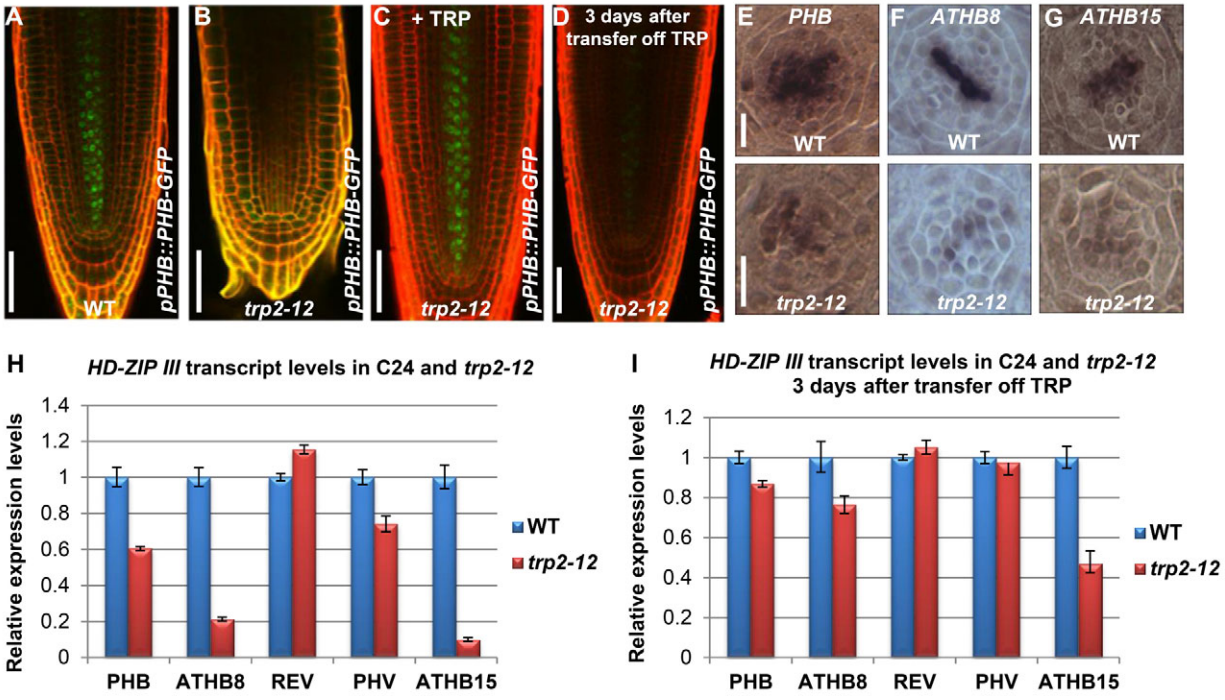

Fig. 2. *HD-ZIP III* gene expression in the *trp2-12* mutant. (A,B) *pPHB::PHB-GFP* in wild type and *trp2-12*. (C,D) *pPHB::PHB-GFP* expression in 6-day-old *trp2-12* plants, which were first germinated and grown on MS medium supplied with L-TRP for 3 days (C), then transferred to medium without L-Trp and analyzed 3 days after transfer. Scale bars: 50 µm. (E-G) *In situ* hybridization with *PHB* (E), *ATHB8* (F) and *ATHB15* (G) mRNA-specific probes on cross sections of the root meristem of wild-type and *trp2-12* mutant seedlings. Scale bars: 10 µm. (H) *PHB*, *ATHB8*, *PHV*, *REV* and *ATHB15* transcript levels in wild-type and *trp2-12* root tips. (I) *PHB*, *ATHB8*, *PHV*, *REV* and *ATHB15* transcript levels in 6-day-old wild-type and *trp2-12* roots germinated on MS plates with L-TRP and transferred to MS plates without L-Trp. The root tips were collected 3 days after transfer off L-Trp. The levels of HD-ZIP III transcripts in *trp2-12* (red columns) are presented as relative values compared with the mean values of wild type (blue columns). ACTIN2 was used as a reference. Data are means ± s.d.

Development (2014) doi:10.1242/dev.103473

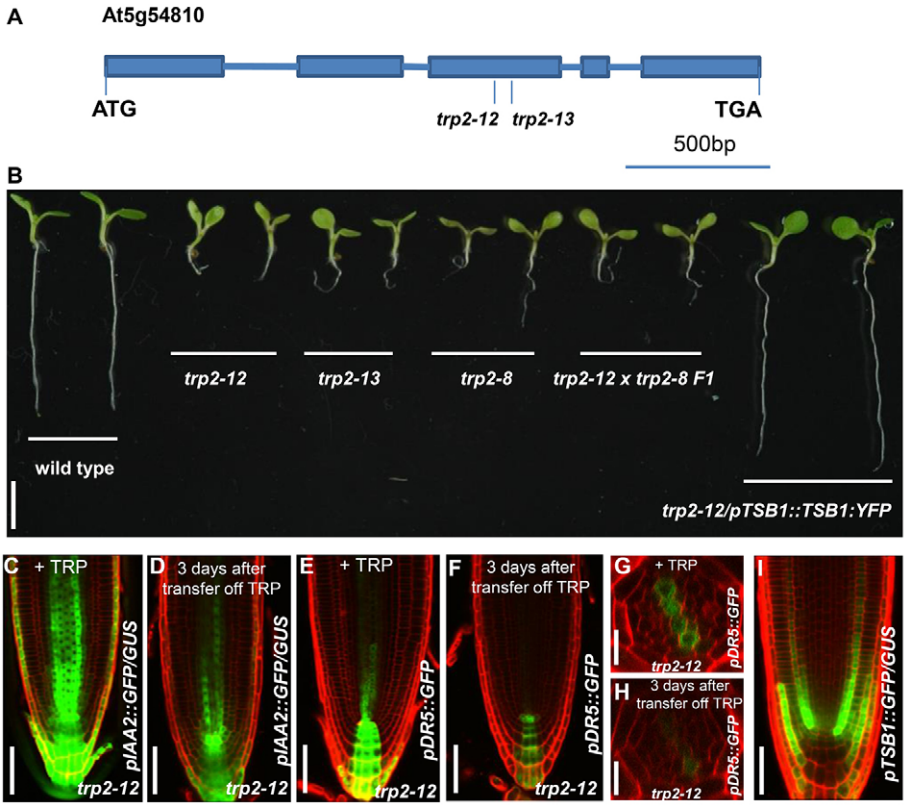

Fig. 3. Cloning of the *trp2-12* mutation, which causes reduced auxin levels in the stele. (A) Schematic view of the intron-exon structure of *TSB1* and sites of the *trp2-12* and *trp2-13* mutations. The *trp2-12* mutation is at position 944 of the coding sequence and causes a C to T change, whereas *trp2-13* is at position 929 of the coding sequence and causes a G to A change. (B) Seedling phenotype of 5-day-old wild-type (C24), *trp2-12*, *trp2-13*, *trp2-8*, *trp2-12*×*trp2-8* F1 progeny and *trp2-12* rescued by *pTSB1:TSB1:YFP*. Scale bar: 0.5 cm. (C) *pIAA2:GFP/GUS* in a 5-day-old *trp2-12* plant germinated on MS medium with L-TRP. (D) *pIAA2:GFP/GUS* in a 3-day-old *trp2-12* plant germinated on MS with L-TRP and transferred to MS medium without L-TRP. (E,G) *pDR5::GFP* in a 5-day-old *trp2-12* plant germinated on MS medium with L-TRP. (F,H) *pDR5::GFP* in a 3-day-old *trp2-12* seedling germinated on MS medium with L-TRP, transferred to medium without L-TRP and grown for a further 3 days. Scale bars: 50 µm for longitudinal and 10 µm for cross sections. (I) *pTSB1::GFP/GUS* expression. Scale bar: 50 µm.

with this, expression of *pACL5::GFPer* (supplementary material Fig. S2A-C) and *pSUC2::GFP* (supplementary material Fig. S1B-D) was indistinguishable between the wild type and the L-Trp supplied *trp2-12* mutant.

This conditional phenotype allowed us to first grow *trp2-12* seedlings on medium supplied with L-Trp for 3 days and then transfer the seedlings to medium lacking L-Trp to observe whether altered *HD-ZIP III* gene expression could be detected prior to the onset of morphological alterations in the root meristem. Reduced *HD-ZIP III* expression levels were observed in *trp2-12* seedling 3 days after transfer, based on qRT-PCR (Fig. 2I), *in situ* hybridization (supplementary material Fig. S2F-K) and *pPHB::PHB-GFP* expression (Fig. 2C,D). The downregulation of *HD-ZIP III* expression occurs prior to obvious developmental changes, as the loss of metaxylem was not seen until 10 days after transfer. These findings show that TSB1-mediated production of tryptophan influences *HD-ZIP III* gene expression and xylem patterning in the root.

Trp-dependent auxin biosynthesis through the TAA1/TAR-YUCCA pathway contributes to vascular patterning

During root development in *Arabidopsis* a distinct auxin maximum occurs at the site of the forming xylem axis (Bishopp et al., 2011). As Trp is a precursor in auxin biosynthesis, we next analyzed whether auxin levels might be altered in *trp2-12* seedlings. As expected, the auxin signaling reporter *pDR5::GFPer* was detected at a reduced level in the root meristem and xylem axis of 5-day-old *trp2-12* seedlings (supplementary material Fig. S1L-N). Furthermore, a similar reduction in the expression levels of auxin-inducible reporters *pDR5::GFPer* and *pIAA2::GFP-GUS* was observed 2-3 days after the transfer of *trp2-12* seedlings from medium containing L-Trp to medium lacking L-Trp (Fig. 3C-H). Importantly, *pDR5::GFPer* expression in the xylem axis was severely diminished after transfer to medium lacking L-Trp (Fig. 3G,H). We conclude that *trp2-12* mutants have reduced auxin levels in the xylem axis.

Screening the *Arabidopsis* eFP Browser (Winter et al., 2007) revealed a complex expression pattern of genes involved in Trp-dependent auxin biosynthesis with several of these genes preferentially expressed in the QC center and its surrounding tissues. We decided to investigate whether *TAA1 (WEI8)*, *TAR2* and *YUCCA* genes might have a function in vascular tissue development, as *TAA1* and *TAR* genes act upstream of *YUCCA* genes in the same biosynthetic pathway (Mashiguchi et al., 2011; Stepanova et al., 2011; Won et al., 2011). Expression of *pTAA1::GFP-TAA1* and *pTAR2::GUS* has previously been detected in two non-overlapping domains of the root meristem. The strongest *pTAA1::GFP-TAA1* expression was detected in the QC and protoxylem as reported before (Fig. 4C). No activity of *pTAR2::GUS* was observed in the meristem region, although pTAR2::GUS expression was detected in the leaf veins (Fig. 4A,B; supplementary material Fig. S3D,E) (Stepanova et al., 2005; Stepanova et al., 2008). We confirmed the lack of *TAR2* expression in the root meristem region by *in situ* mRNA hybridization (supplementary material Fig. S3A-C). Both *pYUCCA8::GFP* and *pYUCCA9::GFP* are highly expressed in the QC, endodermis and cortex precursor cells, and columella (Fig. 4D,E), whereas *pYUCCA3::GUS* expression can be detected in ground tissue cells in the elongation zone (Fig. 4F).

Next, we analyzed the status of xylem formation in the combinatorial mutants for both *TAA1/TAR* and *YUCCA* genes. Interestingly, although PX was properly formed at the peripheral positions of the xylem axis in both *wei8 tar2* double and quintuple *yucca* mutants (lacking *yuc3*, *yuc5*, *yuc7*, *yuc8* and *yuc9*), ectopic PX formation was observed in the central MX position (Fig. 5B,E). We observed a reduction of *pACL5::GFPer* expression in the *wei8*

Development (2014) doi:10.1242/dev.103473

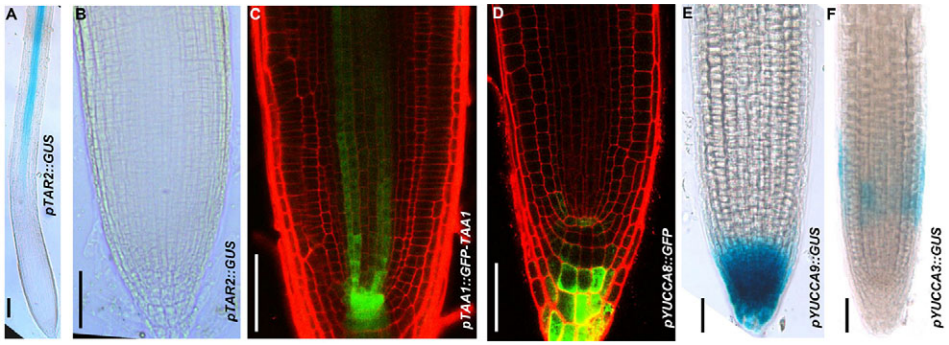

Fig. 4. The expression patterns of auxin biosynthesis genes. (A,B) *pTAR2::GUS* expression (the tip region is shown at higher magnification in B). (C) *pTAA1::GFP-TAA1* expression. (D) *pYUCCA8::GFP* expression. (E) *pYUCCA9::GFP* expression. (F) *pYUCCA3::GUS* expression. Scale bars: 50 µm.

tar2 mutant (Fig. 5J-M). These observations all suggest that TRP-dependent auxin biosynthesis through the TAA1/TAR-YUCCA pathway in the non-vascular tissues is required for MX differentiation in the central domain of the xylem axis in *Arabidopsis* root.

It was recently shown that L-kynurenine (Kyn) acts as an alternative substrate for TAA1/TAR and competitively blocks the activity of these enzymes. Kyn treatment mimics the loss of TAA1/TAR function in *Arabidopsis* and can be used to manipulate TAA1/TAR-dependent auxin biosynthesis (He et al., 2011). To test whether we could pharmacologically block MX differentiation, we treated wild-type and transgenic lines with Kyn (Fig. 5F-I). Following Kyn treatment, we observed a reduction of *pACL5::GFPer* expression (Fig. 6A-C; Fig. 7J). We also observed reduced *pIAA2::GFP/GUS* expression and elevated levels of auxin-downregulated reporter *DII-VENUS* (Brunoud et al., 2012) in the xylem axis, confirming the inhibitory effect of Kyn on auxin biosynthesis (supplementary material Fig. S4A-J). As expected, Kyn treatment also led to the conversion of MX to PX in the central domain of xylem axis, as observed in *wei8 tar2* mutant (Fig. 5B,F). These results suggest that the PX phenotype in *wei8 tar2* and Kyn-treated plants is caused by a reduction of auxin levels in the xylem axis.

To further confirm that reduced auxin levels cause the conversion of MX to PX in the central domain of the xylem axis, we analyzed the effect of Kyn on the two transgenic lines expressing the bacterial auxin biosynthesis gene *iaaH* (Schroder, 1984; Thomashow et al., 1984) in the root meristem (*pTSB1::iaaH*) or QC (*pWOX5::XVE>>iaaH*), respectively. Whereas Kyn treatment caused ectopic PX formation in both the transgenic and wild-type plants, reduced responsiveness to Kyn was observed when seedlings were additionally supplied with indoleacetamide (IAM) or IAM + estradiol (Fig. 5F-I). This suggests that iaaH-mediated endogenous auxin production in the non-vascular tissue can restore sufficient auxin levels for proper MX formation under conditions inhibiting the TAA1/TAR auxin biosynthetic pathway.

Although we confirmed that Trp-dependent auxin biosynthetic enzymes are expressed in the root meristem, it has also been

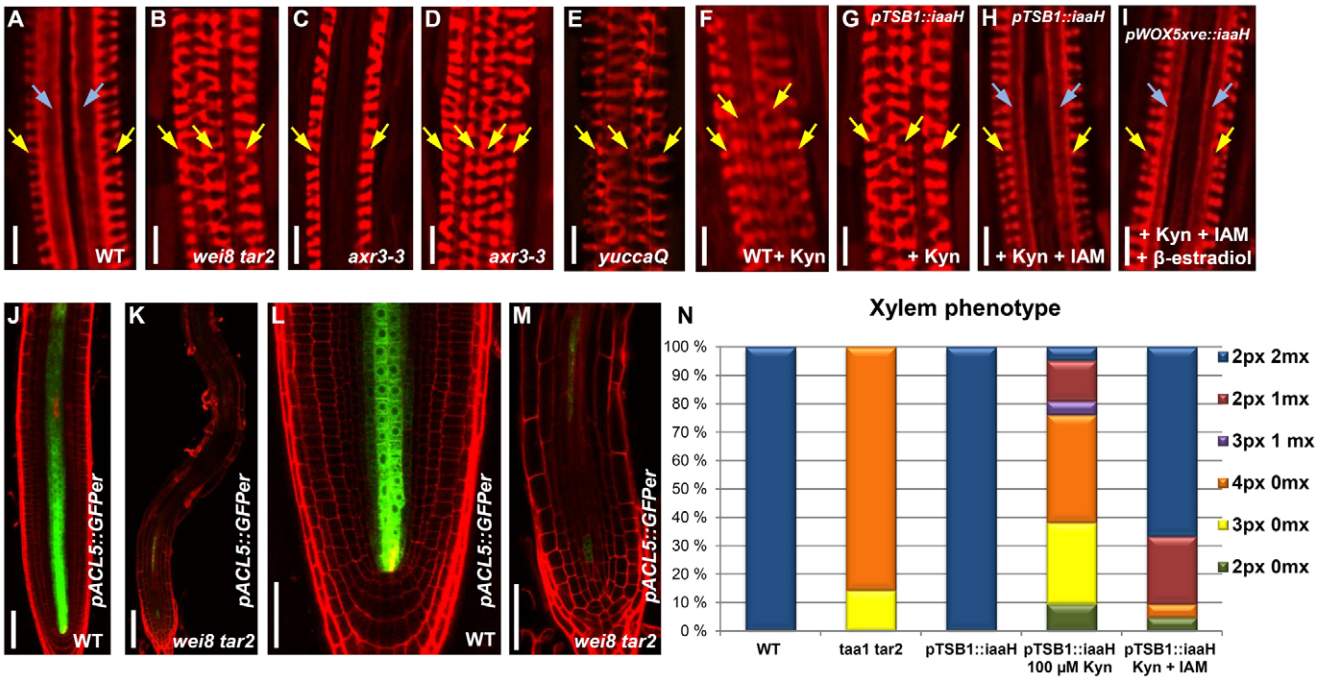

Fig. 5. Auxin biosynthesis by the TAA1/TAR-YUCCA pathway contributes to vascular patterning. (A-I) Basic-fuchsin-stained xylem of wild-type (A), *wei8 tar2* (B), *axr3-3* (C,D), quintuple *yucca* (E) plants, wild-type plants grown on MS supplemented with L-kynurenine (Kyn; F), *pTSB1::iaaH* plants grown with Kyn (G), *pTSB1::iaaH* plants grown with Kyn and IAM (H), *pWOX5xve::iaaH* plants grown with Kyn, IAM and β-estradiol (I). Scale bars: 25 µm. Blue arrows indicate metaxylem and yellow arrows indicate protoxylem. (J-M) *pACL5::GFPer* expression in wild type and in the *wei8 tar2* mutant (the tip region is shown at higher magnification in L and M). Scale bars: 50 µm. (N) Characterization of the xylem phenotype of wild type (*n*=21), *wei8 tar2* (*n*=21), *pTSB1::iaaH* (*n*=21), *pTSB1::iaaH* + Kyn (*n*=21), *pTSB1::iaaH* + Kyn + IAM (*n*=21).

Development (2014) doi:10.1242/dev.103473

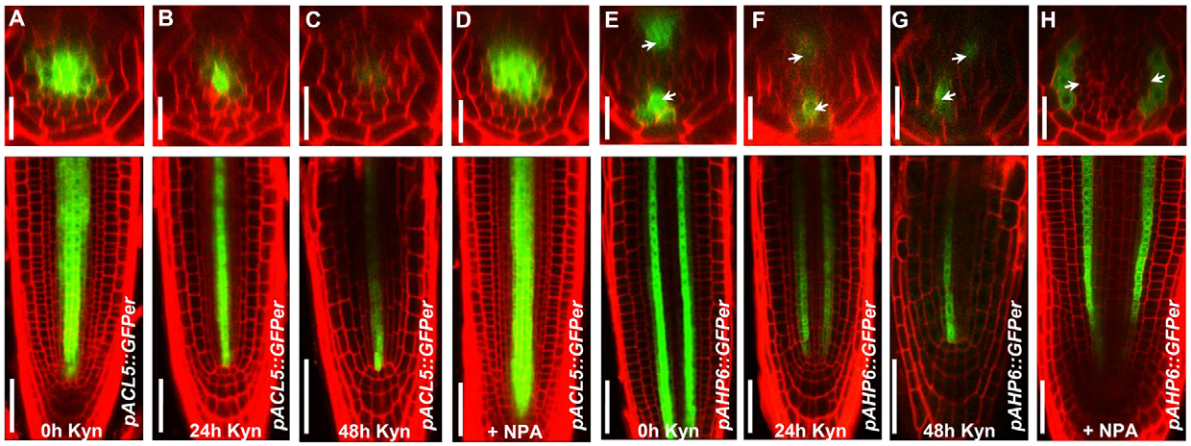

Fig. 6. The different effects of auxin biosynthesis and polar auxin transport on *ACL5* and *AHP6* expression. (A-C) *pACL5::GFPer* in wild-type seedlings germinated on MS without Kyn (A) and transferred to a medium with 100 µM Kyn, and analyzed after 24 (B) and 48 (C) hours of treatment. (D) *pACL5::GFPer* expression in 5-day-old roots grown on a medium with 5 µM NPA. (E-G) *pAHP6::GFPer* in wild-type roots grown on MS medium without Kyn (E), transferred to medium with Kyn and analyzed after 24 (F) and 48 (G) hours. (H) *pAHP6::GFPer* expression in 5-day-old roots grown on medium with 5 µM NPA. Scale bars: 50 µm for longitudinal and 10 µm for cross sections. White arrows indicate protoxylem position.

proposed that several types of phytohormone, including IAA and cytokinin, can be transported from shoot to root through the phloem network (Guo et al., 2005; Overvoorde et al., 2010; Reed et al., 1998). In order to verify whether root-based auxin biosynthesis is sufficient for MX formation, we performed a 'shoot-off' experiment where we followed the xylem formation in the root after cutting the shoot. Four days after removal of the shoot, we still observed proper MX and PX formation, indicating that auxin produced in the QC and its surrounding tissues is sufficient to maintain normal xylem formation (supplementary material Fig. S4K,L).

Examination of the stabilized auxin signaling inhibitor *axr3-3* revealed a lack of MX development, delayed MX formation or an

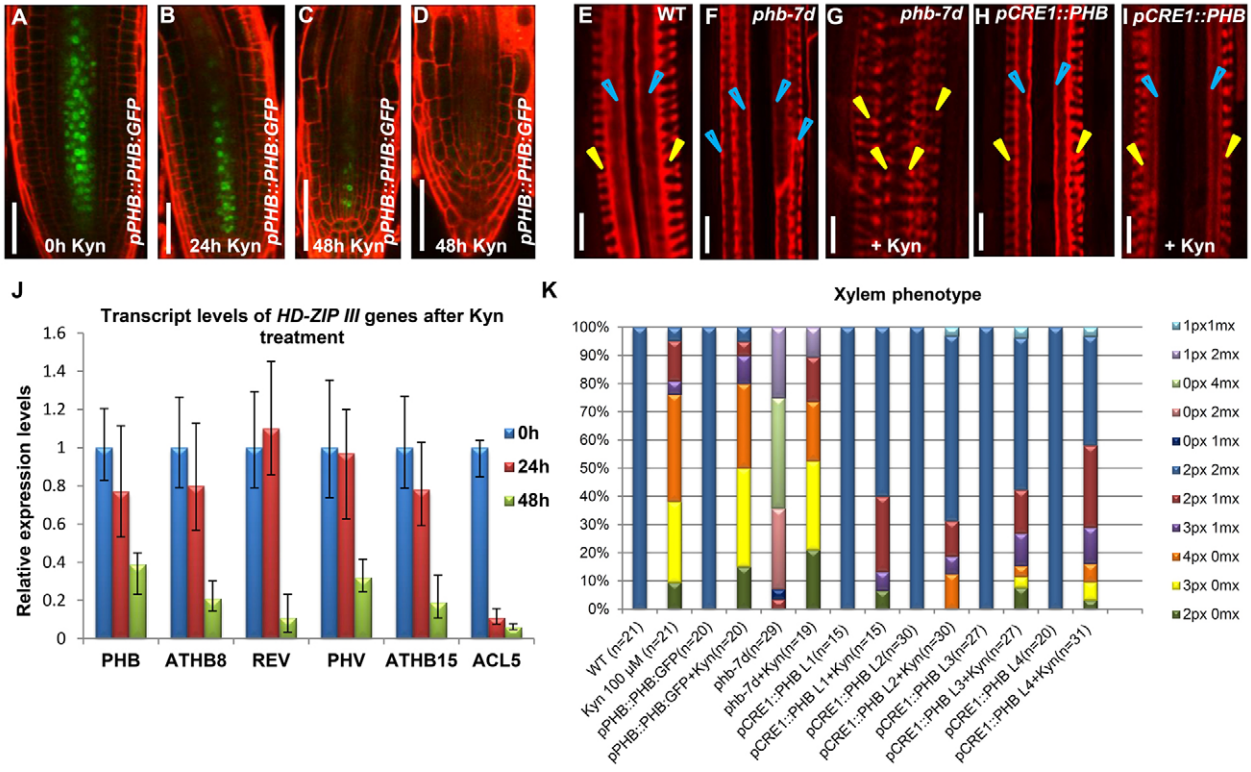

Fig. 7. Auxin biosynthesis influences xylem patterning by regulating the level of *HD-ZIP III* expression. (A-D) *pPHB::PHB:GFP* expression in wild-type plants grown without Kyn and transferred to medium with Kyn for 24 and 48 hours. Scale bars: 50 µm. (E-I) Basic-fuchsin-stained xylem of wild type, *phb-7d*, *phb-7d* + Kyn, *pCRE1::PHB* and *pCRE1::PHB* + Kyn. Scale bars: 25 µm. Blue arrows indicate metaxylem and yellow arrows indicate protoxylem. (J) *PHB*, *ATHB8*, *PHV*, *REV*, *ATHB15* and *ACL5* transcript levels in wild-type root tips grown without Kyn and transferred to a medium with Kyn for 24 and 48 hours. The levels of HD-ZIP III transcripts in Kyn-treated wild-type root tips (red and green columns) are presented as relative values compared with the mean values of untreated wild type (blue columns). ACTIN2 was used as a reference. Data are shown as means ± s.e.m. (K) Characterization of the xylem phenotype in wild type, wild type grown with Kyn, *phb-7d*, *phb-7d* grown with Kyn, and four independent *pCRE1::PHB* lines grown with and without Kyn.

Development (2014) doi:10.1242/dev.103473

all PX phenotype (10/17 developed extra PX; Fig. 5C,D), providing further evidence that auxin biosynthesis and auxin signaling is required for MX differentiation.

The relationship between auxin biosynthesis and auxin transport during root procambial development

Recently it was shown that PAT generates an auxin response maximum at the PX position of the xylem axis and that this auxin maximum is required for the correct expression of *AHP6*, an inhibitor of cytokinin signaling promoting PX differentiation. Genetic and pharmacological inhibition of PAT results in the loss of PX but MX formation is not affected, indicating a differential requirement of PAT between the two xylem domains (Bishopp et al., 2011). By contrast, the *trp2-12*, *wei8 tar2* and quintuple *yucca* mutant with reduced auxin biosynthesis failed to develop MX but showed normal PX development.

To further analyze the differential effects of auxin biosynthesis and polar auxin transport on xylem development, we assayed the expression of *pIAA2::GFP/GUS*, *pAHP6::GFPer* and *pACL5::GFPer* after *N*-1-naphthylphthalamic acid (NPA) and Kyn treatment (Fig. 6 and supplementary material Fig. S4A-H). Bishopp et al. demonstrated that blocking of PAT by NPA results in a complete loss of *pIAA2::GFP/GUS* expression in the entire stele, loss of *pAHP6::GFPer* expression in the PX position and expansion of the signal in the pericycle (Bishopp et al., 2011) (Fig. 6H). However, we were able to demonstrate that the expression of the MX marker *pACL5::GFPer* was not altered after NPA treatment (Fig. 6D). By contrast, Kyn treatment did not affect the expression pattern of *pAHP6::GFPer* (Fig. 6F,G) but caused a reduction in *pACL5::GFPer* expression levels (Fig. 6B,C).

Auxin biosynthesis and auxin signaling promotes *HD-ZIP III* expression in the root meristem

After having shown that auxin biosynthesis is required for MX development, we next tested whether Trp-dependent auxin biosynthesis is required for expression of the *HD-ZIP III* genes. A qRT-PCR assay revealed reduced expression of *PHB*, *AtHB8* and *AtHB15* 24 hours after Kyn treatment of wild-type seedlings, but slightly elevated levels of *REV*; within 48 hours of treatment, expression of all five *HD-ZIP III* genes was reduced (Fig. 7J). Furthermore, *pPHB::PHB-GFP* expression levels were reduced after Kyn treatment (Fig. 7A-D). Because *HD-ZIP III* genes are negatively regulated by miRNA165/166, we analyzed whether Kyn treatment altered the expression of *miRNA165/6*; however, no change in the promoter activity of either miRNA165A or miRNA166B was observed (supplementary material Fig. S5A-F).

To verify that auxin-regulated high levels of *HD-ZIP III* expression are required for MX development, we assayed transgenic lines expressing *PHB* under the control of the auxin-insensitive *pCRE1* promoter (supplementary material Fig. S6). *pCRE1::PHB*-expressing lines developed a normal xylem axis (Fig. 7H) but the seedlings were partially resistant to Kyn; fewer seedlings (<15%) developed ectopic PX in the MX position (Fig. 7I,K). Furthermore, we examined whether the ectopic MX phenotype of the *phb7-d* mutant, which escapes downregulation by miRNA165/166, could be reversed by Kyn treatment (Fig. 7F,G,K). Although we were not able to fully restore the wild-type xylem axis pattern (two marginal PX and two central MX files; Fig. 7E), partial rescue of PX development was observed in *phb7d* mutants (14/19 develop two or more PX files; Fig. 7G,K), indicating that auxin biosynthesis influences xylem patterning by regulating the level of *HD-ZIP III* expression.

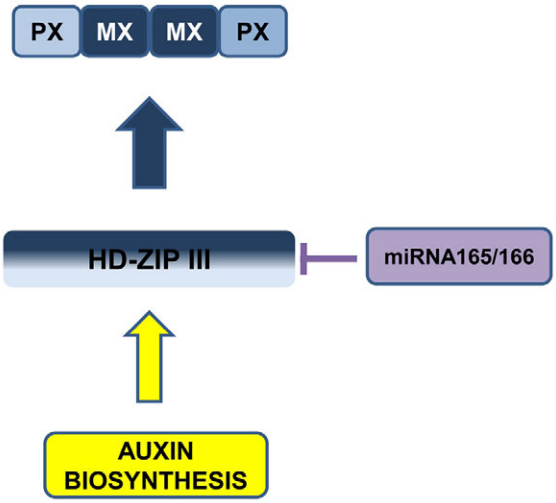

Fig. 8. TRP-dependent auxin biosynthesis is required for HD-ZIP III-mediated metaxylem formation.

DISCUSSION

Various developmental processes depend on the establishment and maintenance of local auxin maxima by PAT and auxin biosynthesis (Cheng et al., 2007; Ikeda et al., 2009; Ljung et al., 2005; Stepanova et al., 2008; Tao et al., 2008; Vanneste and Friml, 2009).

Here we provide evidence that Trp-dependent auxin biosynthesis through the TAA1/TAR-YUCCA pathway is required for HD-ZIP III-mediated MX formation in the xylem axis of *Arabidopsis* roots. Our data further suggest that both processes, PAT and auxin biosynthesis, are required for proper xylem patterning, but that they might have different roles during xylem patterning. PAT specifies PX formation at the xylem axis periphery whereas auxin biosynthesis is required for MX differentiation in the center of the xylem axis (Fig. 8).

Trp is believed to be the main precursor of IAA biosynthesis in plants and is synthesized from chorismate through several catalytic steps (Ljung, 2013; Radwanski and Last, 1995). The final step, the conversion of indole-3-glycerol phosphate to Trp, is catalyzed by an enzyme complex consisting of the TRYPTOPHAN SYNTHASE α- and β-subunits (Barczak et al., 1995; Last et al., 1991). By examining two novel loss-of-function alleles of the TSB1/TRP2 β-subunit, we revealed that TSB1-mediated Trp synthesis participates in the generation of auxin maxima in the root tip, although previous studies detected no altered active auxin levels in *trp2*-mutant seedlings (Last et al., 1991; Normanly et al., 1993; Radwanski and Last, 1995). This discrepancy might be due to local changes in auxin levels having minimal impact on total auxin levels.

Furthermore, *trp2-12* mutants show a misspecification of xylem identity in the central domain of the stele, where MX elements are normally formed. This phenotype could be rescued by externally supplying L-tryptophan.

Similar xylem patterning defects were observed in seedlings in which Trp-dependent auxin biosynthesis was genetically or pharmacologically impaired. Both the double *taa1(wei8)/tar2* and quintuple *yuc3*, *5*, *7*, *8*, *9* mutant, as well as Kyn-treated wild-type seedlings, form ectopic PX instead of MX in the center of the xylem axis, whereas the formation of PX in the peripheral xylem is not altered. Consistent with the xylem phenotypes, expression of the metaxylem marker *ACL5* was downregulated under conditions inhibiting Trp-dependent auxin biosynthesis, whereas expression of the protoxylem marker *AHP6* was still retained. By expressing the bacterial auxin biosynthesis gene *iaaH* in the root meristem, we were

Development (2014) doi:10.1242/dev.103473

able to render xylem patterning resistant to Kyn treatment. This indicates that auxin biosynthesis is required for proper MX formation.

Surprisingly, reporter gene analysis revealed that *TSB1*, *TAA1* and the analyzed *YUCCA* genes are expressed in tissues surrounding the vascular cylinder in the root meristem. Only *TAA1* is additionally expressed in the vascular tissue (He et al., 2011; Stepanova et al., 2008). Based on the expression pattern of the tested genes, it appears that Trp synthesis and Trp-dependent auxin biosynthesis occur in the QC and its surrounding tissues – the ground tissue initials and columella. Furthermore, QC-specific expression of *iaaH* can rescue metaxylem formation in Kyn-treated roots, indicating that auxin produced in non-vascular tissue regulates xylem patterning.

Recently, it has been shown that PAT is required to establish an auxin response maximum at the periphery of the xylem axis, which is needed for PX (Bishopp et al., 2011) but not for MX differentiation. As shown by Bishopp et al., after polar auxin transport inhibition by NPA the auxin-inducible reporter *pIAA2::GFP/GUS* signal disappeared from the xylem axis and became radially symmetric in the pericycle and outer tissues, indicating that auxin signaling is attenuated in the stele under NPA treatment (Bishopp et al., 2011). However, NPA treatment also results in the disappearance of the auxin-downregulated reporter DII-VENUS in the same region (Santuari et al., 2011), suggesting that NPA treatment increases the auxin level in the whole vascular tissue. As reported before (Brunoud et al., 2012), the expression pattern of DII-VENUS is complementary with those of auxin signaling markers, such as DR5 and IAA2. However, under NPA treatment both IAA2 and DII-Venus expression result in the similar pattern. The similar behavior of IAA2, an output of the auxin response pathway, and DII-Venus, a target for auxin interaction that triggers its degradation, after NPA treatment raises the possibility of a feedback loop that currently remains elusive and might involve some additional levels of regulation in MX formation in the central xylem. Alternatively, it is possible that another unknown auxin-independent pathway, which is not visible in the wild-type condition, enhances the HD-ZIP III expression in MX under NPA treatment specifically, and this retains MX formation under NPA treatment. Surprisingly, in this work we discovered that MX differentiation in the central xylem domain depends on auxin biosynthesis whereas genetic and pharmacological interference with auxin production hardly affects peripheral PX specification. Although certain developmental processes, such as leaf formation and root hair positioning, require the combined action of both local auxin biosynthesis and PAT (Cheng et al., 2007; Ikeda et al., 2009) it was surprising to find that Trp-dependent auxin biosynthesis and PAT have different roles in xylem patterning. How the root-based auxin biosynthesis contributes to the creation of an auxin maximum and specifically regulates MX differentiation remains elusive. Because the inhibition of PIN-mediated auxin transport affects xylem formation only in the peripheral PX position, local auxin accumulation in the central xylem position might be regulated primarily by a PIN-independent mechanism, which would be easily affected by local auxin levels.

Xylem cell fate has been shown to be determined by the HD-ZIP III transcription factors in a dose-dependent manner; high expression levels specify metaxylem fate, whereas low levels specify protoxylem (Carlsbecker et al., 2010). Several reports indicate that AtHB8 is induced by auxin in the vasculature and might play a role in PX differentiation (Bishopp et al., 2011). Here, we show that Trp-dependent auxin biosynthesis promotes the expression of most HD-ZIP III genes in the root, revealing a novel mechanism regulating these transcription factors during vascular development. Evidence that auxin biosynthesis influences xylem patterning by regulating HD-ZIP III gene expression is provided by the *phb-7d* gain-of-function mutant that expresses high levels of miR165/6-resistant PHB transcript and forms ectopic MX (Carlsbecker et al., 2010); blocking auxin biosynthesis in this mutant causes the conversion of MX to PX. However, in seedlings expressing *PHB* under the control of the auxin-insensitive *pCRE1* promoter, interfering with auxin synthesis has little effect on xylem patterning. Despite residual low HD-ZIP III expression levels, *trp2-12* mutants often lack xylem in the center of the stele, whereas the *wei8 tar2* and quintuple *yucca* mutants develop an all PX xylem axis. This phenotypic difference suggests that TSB1-mediated Trp synthesis also promotes xylem differentiation by an auxin-independent mechanism downstream of the HD-ZIP IIIs or by post-transcriptionally regulating them.

It has been shown that REV is able to stimulate auxin biosynthesis by regulating TAA1 and YUC5 in the shoot (Brandt et al., 2012). Therefore, it is likely that specific feedback mechanisms regulate auxin biosynthesis and HD-ZIP III expression in the root to control vascular patterning.

MATERIALS AND METHODS

Plant materials and growth conditions

The *Arabidopsis thaliana* accessions C24 and Col-0 were used in all experiments. The mutants and transgenic marker lines were obtained as follows: *axr3-3* (Leyser et al., 1996), *phb-7d* (Carlsbecker et al., 2010), *pDR5rev::GFP* (Friml et al., 2003), *pAHP6::GFPer* (Mähönen et al., 2006), *pAtHB8::GFP*, *pPHB::PHB:GFP*, *pMIR165a::GFP* (Carlsbecker et al., 2010), *pAtSUC2::GFP* (Imlau et al., 1999), *pIAA2::GFP/GUS* (Bishopp et al., 2011), *DII-Venus* (Brunoud et al., 2012). *wei8-1*$^{+/-}$ *tar2-1*$^{-/-}$ (Stepanova et al., 2008) and *trp2-8* (Barczak et al., 1995) were described previously and obtained from the *Arabidopsis* Stock Centre. The genotypes of the mutants were verified using PCR (primers used for genotyping are listed in supplementary material Table S4).

Seeds were sterilized in 70% ethanol and 0.05% Triton X-100, rinsed several times with sterile water, then sown on germination medium containing half-concentration MS (Murashige and Skoog, 1962), 1% sucrose, 0.05% MES [2-(*N*-morpholino) ethanesulfonic acid] and 1% Phytagel. Seeds were then transferred to a growth room at 22°C under a 16-hour light/8-hour dark photoperiod. For treatment and transfer assays, the medium was supplemented with 5 µM *N*-(1-naphthyl)phthalamic acid (NPA; TCI), 20 µM L-tryptophan (Sigma), 100 nM indoleacetamide (IAM; Sigma), 100 µM L-kynurenine (Kyn) (Sigma) or 5 µM 17β-estradiol (Sigma), as indicated in the text.

For anatomical, histological and reporter gene analyses primary roots of 4- to 6-day-old vertically grown seedlings were used.

Screening and map-based cloning of *trp2-12* and *trp2-13* mutants

The *trp2-12* and *trp2-13* mutants were isolated in a genetic screen based on EMS mutagenesis of the mobile phloem marker *pSUC2::GFP* (Imlau et al., 1999) generated previously (Carlsbecker et al., 2010). To map the *TSB1* locus, the *trp2-12* mutant in the C24 background was crossed to Columbia-0 (Col-0) and homozygous mutants were selected in the F2 population for mapping. Genomic DNA was extracted from F2 plants showing the *trp2-12* phenotype and analyzed for co-segregation with respect to cleaved amplified polymorphic sequence (CAPS) and simple sequence length polymorphism (SSLP) markers (Bell and Ecker, 1994; Konieczny and Ausubel, 1993). These markers were derived from the *Arabidopsis* Information Resource (TAIR; http://www.arabidopsis.org). For oligonucleotide sequences, see supplementary material Tables S1 and S2. The rough mapping delimited *trp2-12* to a 300 kb region between the CAPS markers N5-22116697 and N5-22414573 on chromosome 5. A point mutation in the *TSB1* gene (*At5g54810*) was identified when the candidate genes were sequenced (primers used for sequencing are listed in supplementary material Table S3).

Gene expression analyses

To examine the transcript levels of HD-ZIP III genes, root tips from 5-day-old seedlings were collected. Differences in gene expression were measured by real-time PCR as described previously (Carlsbecker et al., 2010).

In situ hybridization experiments

In situ hybridization and probe preparation were performed as in Carlsbecker et al. (Carlsbecker et al., 2010).

Histology and confocal imaging

Transverse sectioning, fuchsin staining and confocal imaging were performed on 5-day-old seedlings as described previously (Mähönen et al., 2000), the confocal analysis was done on a Leica TCS SP5 laser scanning confocal microscope, with the following excitation and emission (Ex/Em) wavelengths: 488 nm/505-530 nm for GFP; 514 nm/525-555 nm for YFP and 488-514 nm/613-679 nm for propidium iodide. GUS staining was performed as described by Miyawaki et al. (Miyawaki et al., 2004). The embedding in plastic and cross sectioning of GUS samples were performed as described previously (Bishopp et al., 2011). The analysis of xylem tissue was carried out with 5-day-old seedlings in chloral hydrate solution (chloral hydrate:glycerol:water 8:1:2).

Generation of transgenic plants

pAHP6::GFPer, *pPHB::PHB-GFP*, *pDR5::GFP*, *pIAA2::GFP/GUS*, *pSUC2::GFP* and *pATHB8::GFPer* markers were introduced into a *trp2-12* mutant background by crossing, and analyses were performed on segregating F2 generations. The transgenic constructs were generated using the Gateway or Multisite Gateway system (Invitrogen) and all were introduced into plants using the floral dip method (Clough and Bent, 1998).

To generate *pTSB1::GFP-GUS*, a 3.15 kb sequence corresponding to the *pTSB1* promoter was amplified from Col-0 genomic DNA with primers 5′-AAAAAGCAGGCTACCATTGAAACAGAAGTGTGGTGATG-3′ (forward) and 5′-AGAAAGCTGGGTTACTGAATGAATCTCTCTCTGAGTC-3′ (reverse) primers, cloned into pDONR(Zeo) and recombined into the destination vector pBGWFS7 (Karimi et al., 2002).

To generate the *pTSB1::TSB1-YFP* construct, a 1.93 kb sequence corresponding to the *TSB1* gene was amplified from Col-0 genomic DNA using primers 5′-AAAAAGCAGGCTATGGCAGCCTCAGGCACCTCTGC-3′ (forward) and 5′-AGAAAGCTGGGTTAACATCAAGATATTTAGCCACTG-3′ (reverse) primers and cloned into pDONR(Zeo). The *pTSB1* promoter was amplified from genomic Col-0 DNA using primers 5′-ATAGAAAAGTTGCCATTGAAACAGAAGTGTGGTGATG-3′ (forward) and 5′-TTGTACAAACTTGTACTGAATGAATCTCTCTCTGAGTC-3′ (reverse) and cloned into pDONRP4-P1R (Invitrogen). The resulting entry clones were recombined together with *YFP* into the multi-site Gateway vector pBm43GW (Karimi et al., 2002).

To generate *pCRE1::PHB*, the entry clones containing *CRE1* promoter (*pCRE1*) (Mähönen et al., 2000) and *PHABULOSA* (*PHB*) gene (Carlsbecker et al., 2010) were recombined into the multisite destination vector pBm43GW.

The *pTSB1* promoter and *iaaH* gene (Blilou et al., 2005) were recombined into the multisite destination vector pBm43GW to produce *pTSB1::iaaH* construct.

The inducible *pWOX5* promoter (Sarkar et al., 2007) and *iaaH* gene were recombined into the multisite destination vector pBm43GW to produce *pWOX5-xve::iaaH*.

For the construction of *pACL5-GFPer*, 2.6 kb of the upstream region of *ACL5* (*At5g19530*) was amplified from Col-0 genomic DNA with the primers 5′-AAGTCGACGGCAAGCTATTCATTAGGC-3′ and 5′-TCGGATCCATCCAAGTTGAGGAGAAGATATAGAGA-3′, digested with *Sal*I and *Bam*HI and placed upstream of the *GAL4:VP16 (GV)* coding region of *pBIN-UAS-GFPer-hssb-GV* (Waki et al., 2013). The resulting construct, *pBIN-UAS-GFPer-pACL5-GV*, was introduced into the *Arabidopsis* Col-0 plant to give the *pACL5-GFPer* reporter line.

Acknowledgements

We thank Mikko Herpola for technical assistance; Sedeer El-Showk for a critical reading of the manuscript; and the *Arabidopsis* Biological Resource Center and the Nottingham *Arabidopsis* Stock Centre for materials.

Competing interests

The authors declare no competing financial interests.

Author contributions

R.U. and S.M. designed and carried out experiments, analyzed data and wrote the paper. Q.C. produced the quintuple *yucca* mutant lines. A.V. and A.C. carried out the EMS mutagenesis screen based on *pAtSUC2::GFP* misexpression. K.N. produced the *pACL5::GFRer* marker line. Y.Z., Y.H. and J.D. participated in experimental design and wrote the manuscript.

Funding

This work was funded by the Academy of Finland, Tekes, the University of Helsinki (Y.H.); Helsinki Graduate Program in Biotechnology and Molecular Biology (R.U.); the European Molecular Biology Organisation [ALTF 450-2007 to J.D.]; and the Japan Society for the Promotion of Science Research Fellowships for Young Scientists (to S.M.).

Supplementary material

Supplementary material available online at
http://dev.biologists.org/lookup/suppl/doi:10.1242/dev.103473/-/DC1

References

Baima, S., Nobili, F., Sessa, G., Lucchetti, S., Ruberti, I. and Morelli, G. (1995). The expression of the Athb-8 homeobox gene is restricted to provascular cells in Arabidopsis thaliana. *Development* **121**, 4171-4182.

Baima, S., Possenti, M., Matteucci, A., Wisman, E., Altamura, M. M., Ruberti, I. and Morelli, G. (2001). The arabidopsis ATHB-8 HD-zip protein acts as a differentiation-promoting transcription factor of the vascular meristems. *Plant Physiol.* **126**, 643-655.

Barczak, A. J., Zhao, J., Pruitt, K. D. and Last, R. L. (1995). 5-Fluoroindole resistance identifies tryptophan synthase beta subunit mutants in Arabidopsis thaliana. *Genetics* **140**, 303-313.

Bell, C. J. and Ecker, J. R. (1994). Assignment of 30 microsatellite loci to the linkage map of Arabidopsis. *Genomics* **19**, 137-144.

Benková, E., Michniewicz, M., Sauer, M., Teichmann, T., Seifertová, D., Jürgens, G. and Friml, J. (2003). Local, efflux-dependent auxin gradients as a common module for plant organ formation. *Cell* **115**, 591-602.

Bishopp, A., Help, H., El-Showk, S., Weijers, D., Scheres, B., Friml, J., Benkova, E., Mähönen, A. P. and Helariutta, Y. (2011). A mutually inhibitory interaction between auxin and cytokinin specifies vascular pattern in roots. *Curr. Biol.* **21**, 917-926.

Blilou, I., Xu, J., Wildwater, M., Willemsen, V., Paponov, I., Friml, J., Heidstra, R., Aida, M., Palme, K. and Scheres, B. (2005). The PIN auxin efflux facilitator network controls growth and patterning in Arabidopsis roots. *Nature* **433**, 39-44.

Brandt, R., Salla-Martret, M., Bou-Torrent, J., Musielak, T., Stahl, M., Lanz, C., Ott, F., Schmid, M., Greb, T., Schwarz, M. et al. (2012). Genome-wide binding-site analysis of REVOLUTA reveals a link between leaf patterning and light-mediated growth responses. *Plant J.* **72**, 31-42.

Brunoud, G., Wells, D. M., Oliva, M., Larrieu, A., Mirabet, V., Burrow, A. H., Beeckman, T., Kepinski, S., Traas, J., Bennett, M. J. et al. (2012). A novel sensor to map auxin response and distribution at high spatio-temporal resolution. *Nature* **482**, 103-106.

Carlsbecker, A., Lee, J. Y., Roberts, C. J., Dettmer, J., Lehesranta, S., Zhou, J., Lindgren, O., Moreno-Risueno, M. A., Vatén, A., Thitamadee, S. et al. (2010). Cell signalling by microRNA165/6 directs gene dose-dependent root cell fate. *Nature* **465**, 316-321.

Chandler, J. W. (2009). Auxin as compère in plant hormone crosstalk. *Planta* **231**, 1-12.

Cheng, Y., Dai, X. and Zhao, Y. (2006). Auxin biosynthesis by the YUCCA flavin monooxygenases controls the formation of floral organs and vascular tissues in Arabidopsis. *Genes Dev.* **20**, 1790-1799.

Cheng, Y., Dai, X. and Zhao, Y. (2007). Auxin synthesized by the YUCCA flavin monooxygenases is essential for embryogenesis and leaf formation in Arabidopsis. *Plant Cell* **19**, 2430-2439.

Cho, M., Lee, S. H. and Cho, H. T. (2007). P-glycoprotein4 displays auxin efflux transporter-like action in Arabidopsis root hair cells and tobacco cells. *Plant Cell* **19**, 3930-3943.

Clough, S. J. and Bent, A. F. (1998). Floral dip: a simplified method for Agrobacterium-mediated transformation of Arabidopsis thaliana. *Plant J.* **16**, 735-743.

Cohen, J. D., Slovin, J. P. and Hendrickson, A. M. (2003). Two genetically discrete pathways convert tryptophan to auxin: more redundancy in auxin biosynthesis. *Trends Plant Sci.* **8**, 197-199.

Donner, T. J., Sherr, I. and Scarpella, E. (2009). Regulation of preprocambial cell state acquisition by auxin signaling in Arabidopsis leaves. *Development* **136**, 3235-3246.

Friml, J., Benková, E., Blilou, I., Wisniewska, J., Hamann, T., Ljung, K., Woody, S., Sandberg, G., Scheres, B., Jürgens, G. et al. (2002). AtPIN4 mediates sink-driven auxin gradients and root patterning in Arabidopsis. *Cell* **108**, 661-673.

Friml, J., Vieten, A., Sauer, M., Weijers, D., Schwarz, H., Hamann, T., Offringa, R. and Jürgens, G. (2003). Efflux-dependent auxin gradients establish the apical-basal axis of Arabidopsis. *Nature* **426**, 147-153.

Friml, J., Vieten, A., Sauer, M., Michniewicz, M., Paciorek, T., Wisniewska, J. and Jurgens, G. (2004). Auxin transport – how cells make a plant. *Acta Physiol. Plant.* **26**, 147-148.

Gälweiler, L., Guan, C., Müller, A., Wisman, E., Mendgen, K., Yephremov, A. and Palme, K. (1998). Regulation of polar auxin transport by AtPIN1 in Arabidopsis vascular tissue. *Science* **282**, 2226-2230.

Geisler, M., Blakeslee, J. J., Bouchard, R., Lee, O. R., Vincenzetti, V., Bandyopadhyay, A., Titapiwatanakun, B., Peer, W. A., Bailly, A., Richards, E. L.

et al. (2005). Cellular efflux of auxin catalyzed by the Arabidopsis MDR/PGP transporter AtPGP1. *Plant J.* **44**, 179-194.
Grieneisen, V. A., Xu, J., Marée, A. F., Hogeweg, P. and Scheres, B. (2007). Auxin transport is sufficient to generate a maximum and gradient guiding root growth. *Nature* **449**, 1008-1013.
Guo, H. S., Xie, Q., Fei, J. F. and Chua, N. H. (2005). MicroRNA directs mRNA cleavage of the transcription factor NAC1 to downregulate auxin signals for arabidopsis lateral root development. *Plant Cell* **17**, 1376-1386.
He, W., Brumos, J., Li, H., Ji, Y., Ke, M., Gong, X., Zeng, Q., Li, W., Zhang, X., An, F. et al. (2011). A small-molecule screen identifies L-kynurenine as a competitive inhibitor of TAA1/TAR activity in ethylene-directed auxin biosynthesis and root growth in Arabidopsis. *Plant Cell* **23**, 3944-3960.
Ikeda, Y., Men, S., Fischer, U., Stepanova, A. N., Alonso, J. M., Ljung, K. and Grebe, M. (2009). Local auxin biosynthesis modulates gradient-directed planar polarity in Arabidopsis. *Nat. Cell Biol.* **11**, 731-738.
Imlau, A., Truernit, E. and Sauer, N. (1999). Cell-to-cell and long-distance trafficking of the green fluorescent protein in the phloem and symplastic unloading of the protein into sink tissues. *Plant Cell* **11**, 309-322.
Izhaki, A. and Bowman, J. L. (2007). KANADI and class III HD-Zip gene families regulate embryo patterning and modulate auxin flow during embryogenesis in Arabidopsis. *Plant Cell* **19**, 495-508.
Jing, Y., Cui, D., Bao, F., Hu, Z., Qin, Z. and Hu, Y. (2009). Tryptophan deficiency affects organ growth by retarding cell expansion in Arabidopsis. *Plant J.* **57**, 511-521.
Karimi, M., Inzé, D. and Depicker, A. (2002). GATEWAY vectors for Agrobacterium-mediated plant transformation. *Trends Plant Sci.* **7**, 193-195.
Konieczny, A. and Ausubel, F. M. (1993). A procedure for mapping Arabidopsis mutations using co-dominant ecotype-specific PCR-based markers. *Plant J.* **4**, 403-410.
Korasick, D. A., Enders, T. A. and Strader, L. C. (2013). Auxin biosynthesis and storage forms. *J. Exp. Bot.* **64**, 2541-2555.
Last, R. L. and Fink, G. R. (1988). Tryptophan-requiring mutants of the plant Arabidopsis thaliana. *Science* **240**, 305-310.
Last, R. L., Bissinger, P. H., Mahoney, D. J., Radwanski, E. R. and Fink, G. R. (1991). Tryptophan mutants in Arabidopsis: the consequences of duplicated tryptophan synthase beta genes. *Plant Cell* **3**, 345-358.
Leyser, H. M., Pickett, F. B., Dharmasiri, S. and Estelle, M. (1996). Mutations in the AXR3 gene of Arabidopsis result in altered auxin response including ectopic expression from the SAUR-AC1 promoter. *Plant J.* **10**, 403-413.
Ljung, K. (2013). Auxin metabolism and homeostasis during plant development. *Development* **140**, 943-950.
Ljung, K., Hull, A. K., Celenza, J., Yamada, M., Estelle, M., Normanly, J. and Sandberg, G. (2005). Sites and regulation of auxin biosynthesis in Arabidopsis roots. *Plant Cell* **17**, 1090-1104.
Mähönen, A. P., Bonke, M., Kauppinen, L., Riikonen, M., Benfey, P. N. and Helariutta, Y. (2000). A novel two-component hybrid molecule regulates vascular morphogenesis of the Arabidopsis root. *Genes Dev.* **14**, 2938-2943.
Mähönen, A. P., Higuchi, M., Tormakangas, K., Miyawaki, K., Pischke, M. S., Sussman, M. R., Helariutta, Y. and Kakimoto, T. (2006). Cytokinins regulate a bidirectional phosphorelay network in Arabidopsis. *Curr. Biol.* **16**, 1116-1122.
Mashiguchi, K., Tanaka, K., Sakai, T., Sugawara, S., Kawaide, H., Natsume, M., Hanada, A., Yaeno, T., Shirasu, K., Yao, H. et al. (2011). The main auxin biosynthesis pathway in Arabidopsis. *Proc. Natl. Acad. Sci. USA* **108**, 18512-18517.
Mattsson, J., Ckurshumova, W. and Berleth, T. (2003). Auxin signaling in Arabidopsis leaf vascular development. *Plant Physiol.* **131**, 1327-1339.
Miyashima, S., Koi, S., Hashimoto, T. and Nakajima, K. (2011). Non-cell-autonomous microRNA165 acts in a dose-dependent manner to regulate multiple differentiation status in the Arabidopsis root. *Development* **138**, 2303-2313.
Miyawaki, K., Matsumoto-Kitano, M. and Kakimoto, T. (2004). Expression of cytokinin biosynthetic isopentenyltransferase genes in Arabidopsis: tissue specificity and regulation by auxin, cytokinin, and nitrate. *Plant J.* **37**, 128-138.
Müller, A. and Weiler, E. W. (2000). Indolic constituents and indole-3-acetic acid biosynthesis in the wild-type and a tryptophan auxotroph mutant of Arabidopsis thaliana. *Planta* **211**, 855-863.
Muñiz, L., Minguet, E. G., Singh, S. K., Pesquet, E., Vera-Sirera, F., Moreau-Courtois, C. L., Carbonell, J., Blázquez, M. A. and Tuominen, H. (2008). ACAULIS5 controls Arabidopsis xylem specification through the prevention of premature cell death. *Development* **135**, 2573-2582.
Murashige, T. and Skoog, F. (1962). A revised medium for rapid growth and bio assays with tobacco tissue cultures. *Physiol. Plantarum* **15**, 473-497.
Normanly, J., Cohen, J. D. and Fink, G. R. (1993). Arabidopsis thaliana auxotrophs reveal a tryptophan-independent biosynthetic pathway for indole-3-acetic acid. *Proc. Natl. Acad. Sci. USA* **90**, 10355-10359.
Ostin, A., Ilic, N. and Cohen, J. D. (1999). An in vitro system from maize seedlings for tryptophan-independent indole-3-acetic acid biosynthesis. *Plant Physiol.* **119**, 173-178.
Overvoorde, P., Fukaki, H. and Beeckman, T. (2010). Auxin control of root development. *Cold Spring Harb. Perspect. Biol.* **2**, a001537.
Petersson, S. V., Johansson, A. I., Kowalczyk, M., Makoveychuk, A., Wang, J. Y., Moritz, T., Grebe, M., Benfey, P. N., Sandberg, G. and Ljung, K. (2009). An auxin gradient and maximum in the Arabidopsis root apex shown by high-resolution cell-specific analysis of IAA distribution and synthesis. *Plant Cell* **21**, 1659-1668.
Petrásek, J., Mravec, J., Bouchard, R., Blakeslee, J. J., Abas, M., Seifertová, D., Wisniewska, J., Tadele, Z., Kubes, M., Covanová, M. et al. (2006). PIN proteins perform a rate-limiting function in cellular auxin efflux. *Science* **312**, 914-918.
Radwanski, E. R. and Last, R. L. (1995). Tryptophan biosynthesis and metabolism: biochemical and molecular genetics. *Plant Cell* **7**, 921-934.
Reed, R. C., Brady, S. R. and Muday, G. K. (1998). Inhibition of auxin movement from the shoot into the root inhibits lateral root development in Arabidopsis. *Plant Physiol.* **118**, 1369-1378.
Santuari, L., Scacchi, E., Rodriguez-Villalon, A., Salinas, P., Dohmann, E. M., Brunoud, G., Vernoux, T., Smith, R. S. and Hardtke, C. S. (2011). Positional information by differential endocytosis splits auxin response to drive Arabidopsis root meristem growth. *Curr. Biol.* **21**, 1918-1923.
Sarkar, A. K., Luijten, M., Miyashima, S., Lenhard, M., Hashimoto, T., Nakajima, K., Scheres, B., Heidstra, R. and Laux, T. (2007). Conserved factors regulate signalling in Arabidopsis thaliana shoot and root stem cell organizers. *Nature* **446**, 811-814.
Sauer, M., Robert, S. and Kleine-Vehn, J. (2013). Auxin: simply complicated. *J. Exp. Bot.* **64**, 2565-2577.
Scarpella, E., Marcos, D., Friml, J. and Berleth, T. (2006). Control of leaf vascular patterning by polar auxin transport. *Genes Dev.* **20**, 1015-1027.
Schroder, J. (1984). The T-region of Ti-plasmids codes for an enzyme of auxin biosynthesis. *H.-S. Z. Physiol. Chem.* **365**, 217.
Schuetz, M., Smith, R. and Ellis, B. (2013). Xylem tissue specification, patterning, and differentiation mechanisms. *J. Exp. Bot.* **64**, 11-31.
Sorefan, K., Girin, T., Liljegren, S. J., Ljung, K., Robles, P., Galván-Ampudia, C. S., Offringa, R., Friml, J., Yanofsky, M. F. and Østergaard, L. (2009). A regulated auxin minimum is required for seed dispersal in Arabidopsis. *Nature* **459**, 583-586.
Stadler, R., Wright, K. M., Lauterbach, C., Amon, G., Gahrtz, M., Feuerstein, A., Oparka, K. J. and Sauer, N. (2005). Expression of GFP-fusions in Arabidopsis companion cells reveals non-specific protein trafficking into sieve elements and identifies a novel post-phloem domain in roots. *Plant J.* **41**, 319-331.
Stepanova, A. N., Hoyt, J. M., Hamilton, A. A. and Alonso, J. M. (2005). A Link between ethylene and auxin uncovered by the characterization of two root-specific ethylene-insensitive mutants in Arabidopsis. *Plant Cell* **17**, 2230-2242.
Stepanova, A. N., Robertson-Hoyt, J., Yun, J., Benavente, L. M., Xie, D. Y., Dolezal, K., Schlereth, A., Jürgens, G. and Alonso, J. M. (2008). TAA1-mediated auxin biosynthesis is essential for hormone crosstalk and plant development. *Cell* **133**, 177-191.
Stepanova, A. N., Yun, J., Robles, L. M., Novak, O., He, W., Guo, H., Ljung, K. and Alonso, J. M. (2011). The Arabidopsis YUCCA1 flavin monooxygenase functions in the indole-3-pyruvic acid branch of auxin biosynthesis. *Plant Cell* **23**, 3961-3973.
Strader, L. C. and Bartel, B. (2008). A new path to auxin. *Nat. Chem. Biol.* **4**, 337-339.
Sugawara, S., Hishiyama, S., Jikumaru, Y., Hanada, A., Nishimura, T., Koshiba, T., Zhao, Y., Kamiya, Y. and Kasahara, H. (2009). Biochemical analyses of indole-3-acetaldoxime-dependent auxin biosynthesis in Arabidopsis. *Proc. Natl. Acad. Sci. USA* **106**, 5430-5435.
Swarup, K., Benková, E., Swarup, R., Casimiro, I., Péret, B., Yang, Y., Parry, G., Nielsen, E., De Smet, I., Vanneste, S. et al. (2008). The auxin influx carrier LAX3 promotes lateral root emergence. *Nat. Cell Biol.* **10**, 946-954.
Tao, Y., Ferrer, J. L., Ljung, K., Pojer, F., Hong, F., Long, J. A., Li, L., Moreno, J. E., Bowman, M. E., Ivans, L. J. et al. (2008). Rapid synthesis of auxin via a new tryptophan-dependent pathway is required for shade avoidance in plants. *Cell* **133**, 164-176.
Thomashow, L. S., Reeves, S. and Thomashow, M. F. (1984). Crown gall oncogenesis – evidence that a t-dna gene from the agrobacterium-ti plasmid ptia6 encodes an enzyme that catalyzes synthesis of indoleacetic-acid. *Proc. Natl. Acad. Sci. Biol.* **81**, 5071-5075.
Vanneste, S. and Friml, J. (2009). Auxin: a trigger for change in plant development. *Cell* **136**, 1005-1016.
Waki, T., Miyashima, S., Nakanishi, M., Ikeda, Y., Hashimoto, T. and Nakajima, K. (2013). A GAL4-based targeted activation tagging system in Arabidopsis thaliana. *Plant J.* **73**, 357-367.
Weijers, D. and Jürgens, G. (2005). Auxin and embryo axis formation: the ends in sight? *Curr. Opin. Plant Biol.* **8**, 32-37.
Wenzel, C. L., Schuetz, M., Yu, Q. and Mattsson, J. (2007). Dynamics of MONOPTEROS and PIN-FORMED1 expression during leaf vein pattern formation in Arabidopsis thaliana. *Plant J.* **49**, 387-398.
Winter, D., Vinegar, B., Nahal, H., Ammar, R., Wilson, G. V. and Provart, N. J. (2007). An "Electronic Fluorescent Pictograph" browser for exploring and analyzing large-scale biological data sets. *PLoS ONE* **2**, e718.
Won, C., Shen, X., Mashiguchi, K., Zheng, Z., Dai, X., Cheng, Y., Kasahara, H., Kamiya, Y., Chory, J. and Zhao, Y. (2011). Conversion of tryptophan to indole-3-acetic acid by tryptophan aminotransferases of Arabidopsis and YUCCAs in Arabidopsis. *Proc. Natl. Acad. Sci. USA* **108**, 18518-18523.
Woodward, A. W. and Bartel, B. (2005). Auxin: regulation, action, and interaction. *Ann. Bot.* **95**, 707-735.
Yin, R., Frey, M., Gierl, A. and Glawischnig, E. (2010). Plants contain two distinct classes of functional tryptophan synthase beta proteins. *Phytochemistry* **71**, 1667-1672.
Zhang, R., Wang, B., Ouyang, J., Li, J. and Wang, Y. (2008). Arabidopsis indole synthase, a homolog of tryptophan synthase alpha, is an enzyme involved in the Trp-independent indole-containing metabolite biosynthesis. *J. Integr. Plant Biol.* **50**, 1070-1077.
Zhao, Y. (2010). Auxin biosynthesis and its role in plant development. *Annu. Rev. Plant Biol.* **61**, 49-64.
Zhao, Y. (2012). Auxin biosynthesis: a simple two-step pathway converts tryptophan to indole-3-acetic acid in plants. *Mol. Plant* **5**, 334-338.
Zhao, Y., Hull, A. K., Gupta, N. R., Goss, K. A., Alonso, J., Ecker, J. R., Normanly, J., Chory, J. and Celenza, J. L. (2002). Trp-dependent auxin biosynthesis in Arabidopsis: involvement of cytochrome P450s CYP79B2 and CYP79B3. *Genes Dev.* **16**, 3100-3112.

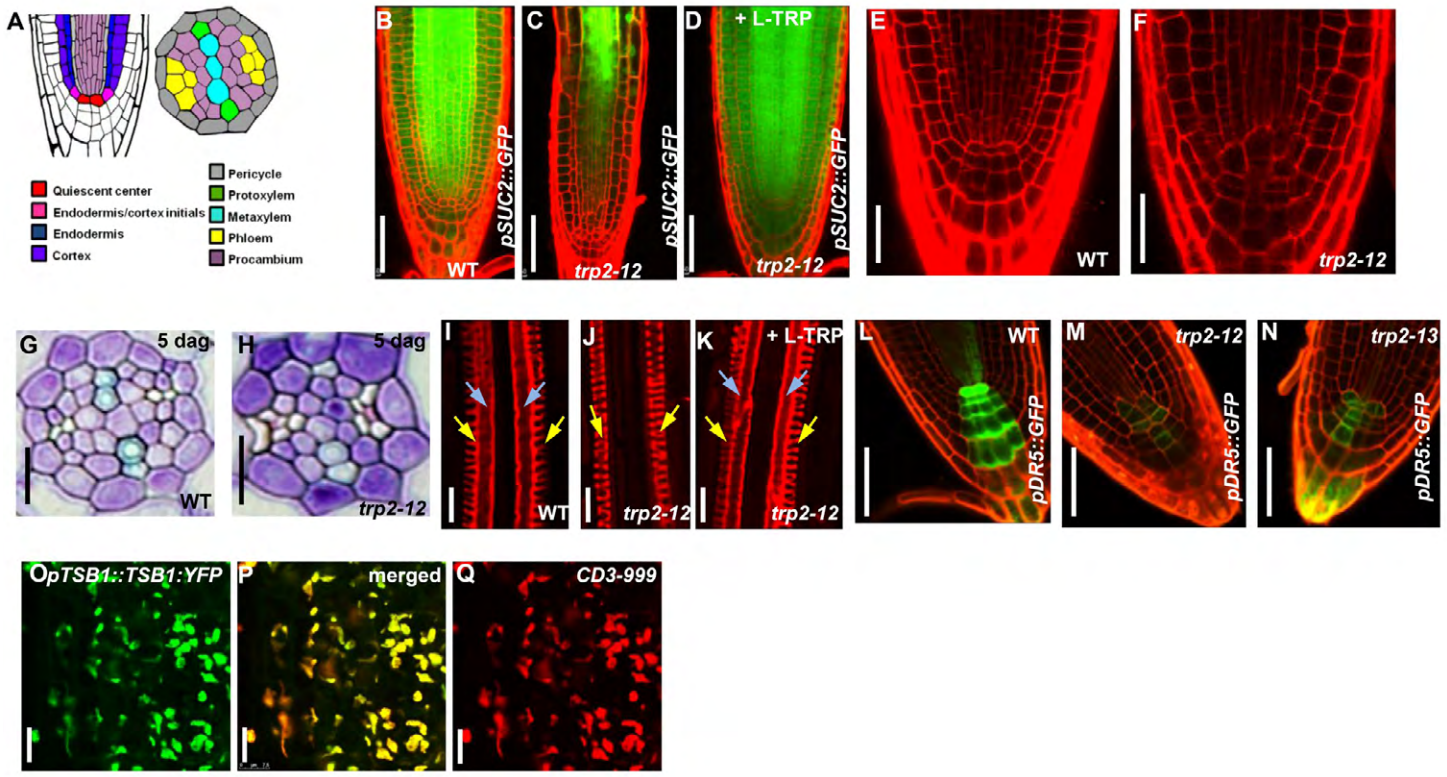

Supplementary Fig. 1. Characterization of *trp2-12* mutant. (A) A schematic representation of the *Arabidopsis* root. (B-D) *pSUC2::GFP* in 5 day-old wild-type (B), *trp2-12* grown without (C) and with L-Trp (D). (Scale bar: 50 µm.). (E,F) Wild-type and *trp2-12* roots stained with propidium iodide (Scale bars: 25 µm). (G,H) Toluidine-blue stained root cross-sections of 5 day-old wild-type and *trp2-12* roots. (Scale bar: 25 µm.). (I-K) Basic fuchsin-stained xylem of 5-day old wild-type (I), *trp2-12* grown without (J) and with L-Trp (K). (Scale bar: 25 µm.) Blue arrows indicate metaxylem and yellow arrows indicate protoxylem. (L-N) *pDR5::GFP* in 5-day old wild-type, *trp2-12* and *trp2-13.* (Scale bar: 50 µm). (O-Q) Subcellular localization of the TSB1 protein to the plastids in the *Arabidopsis* root epidermis. (Scale bars: 7.5 µm).

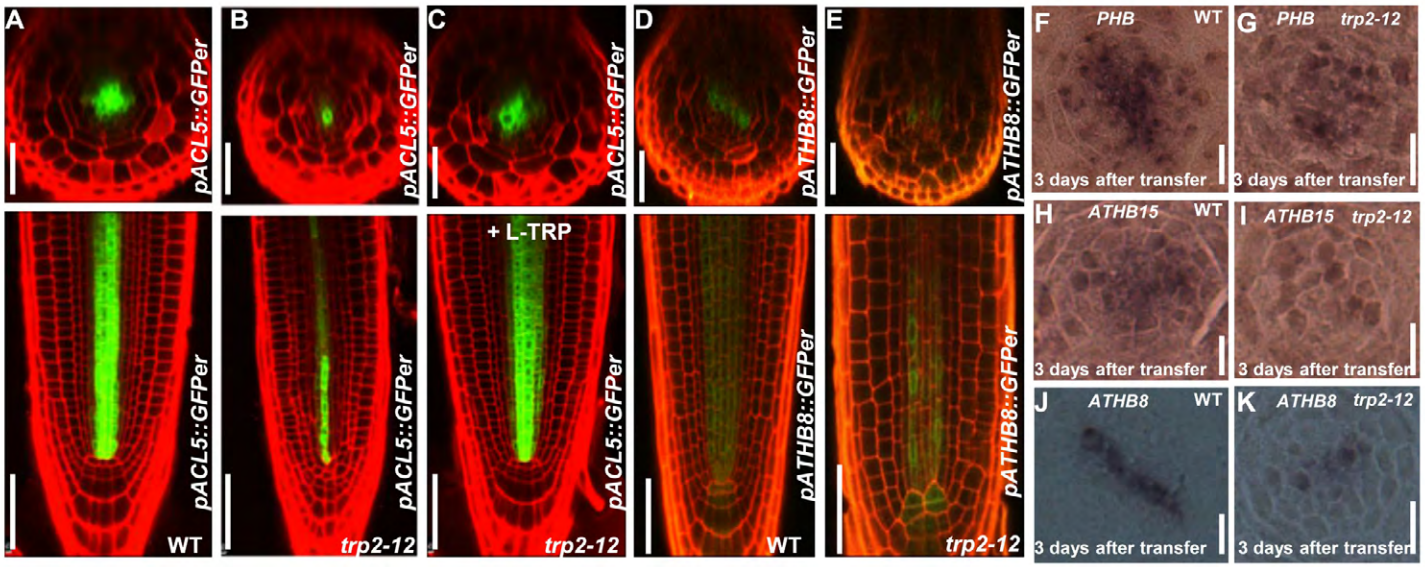

Supplementary Fig. 2. (A-C) *pACL5::GFPer* in 5-day old wild-type and *trp2-12* grown with and without L-TRP. (D,E) *pATHB8::GFP* in 5-day old wild-type and *trp2-12* plants (Scale bar: 50 µm). (F-K) *In situ* hybridization with *PHB, ATHB8* and *ATHB15* mRNA-specific probes on cross sections of the root meristem in the *trp2-12* mutant grown with L-Trp and transferred to a medium without L-Trp. Scale bar: 10 µm).

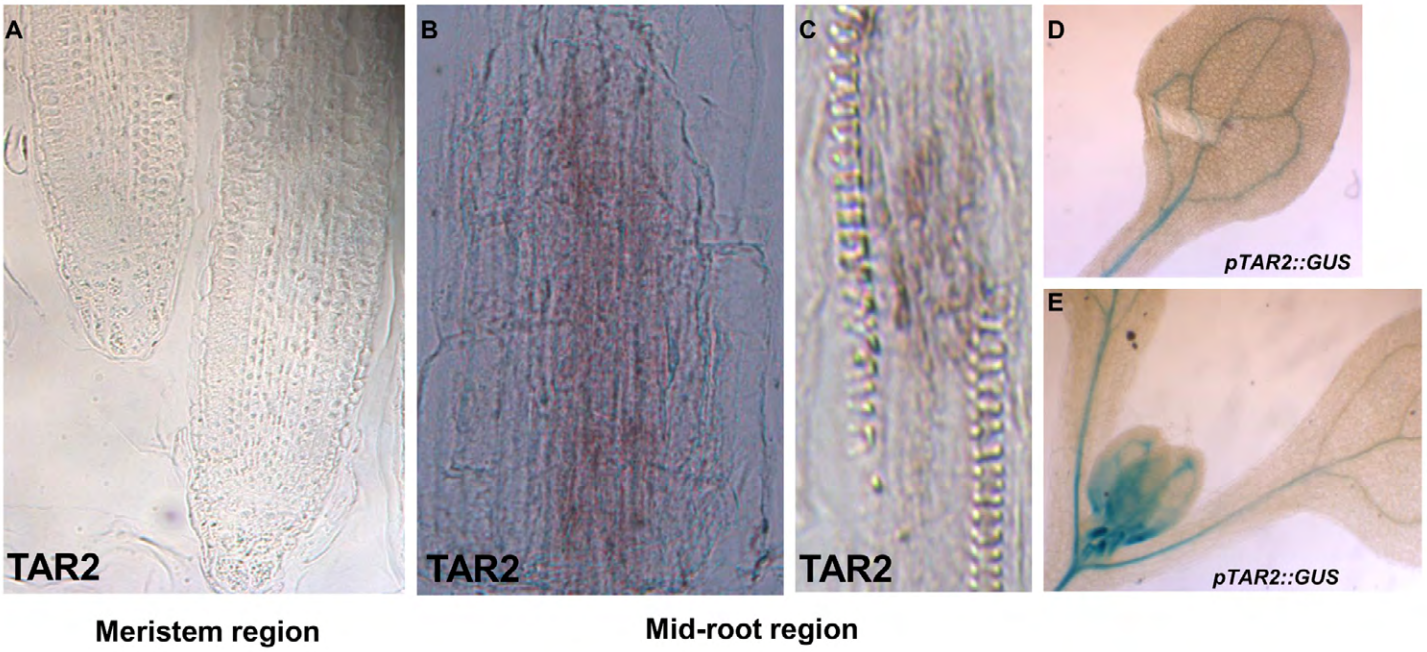

Supplementary Fig. 3. (A-C) TAR2 mRNA-specific probe on longitudinal sections of the root meristem (A) and mid-root region (B,C) of 5 day-old wild-type . (D,E) *pTAR2::GUS* expression in 5-day old leaves.

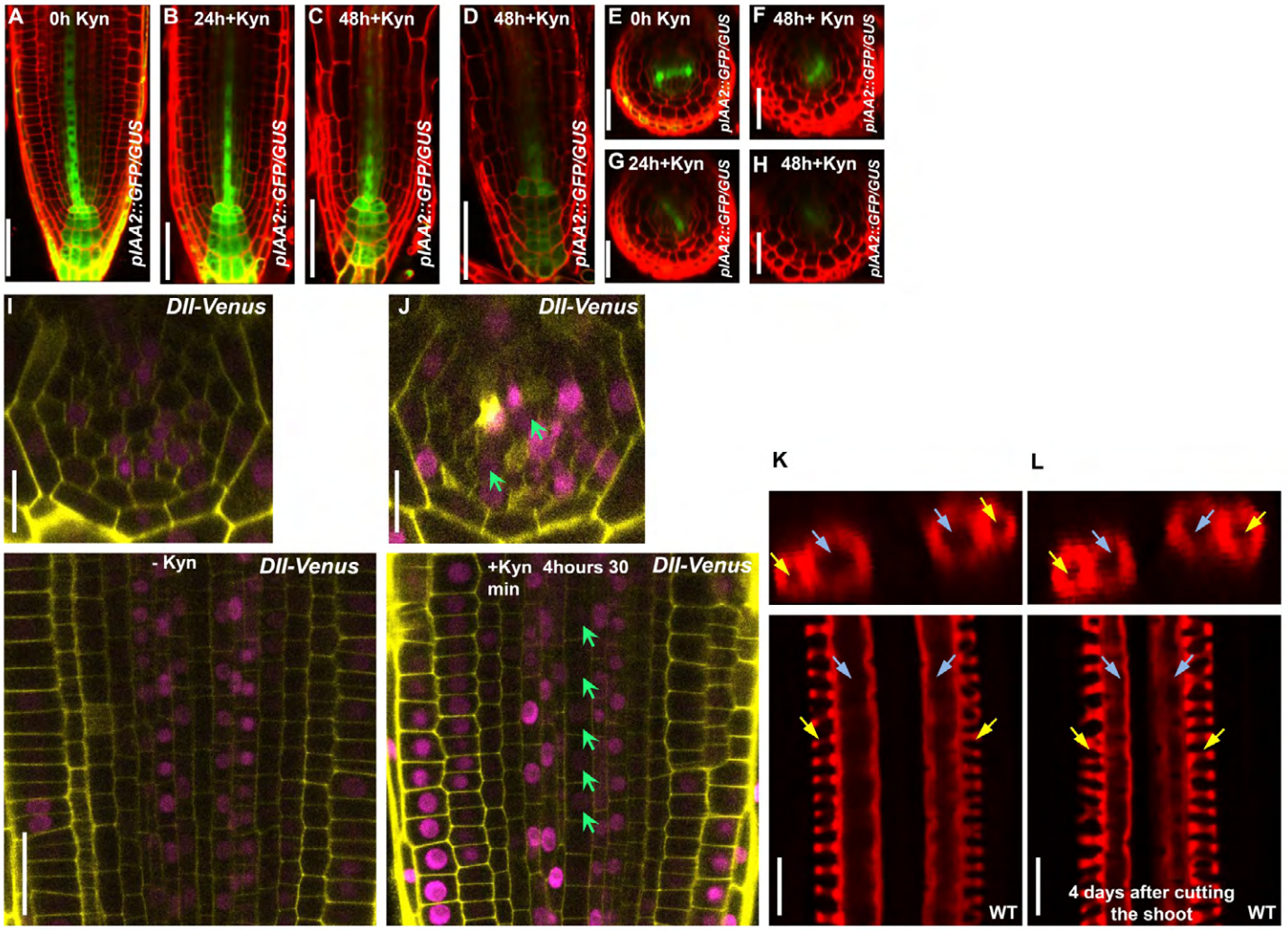

Supplementary Fig. 4. (A-H) *pIAA2::GFP/GUS* in 5-day old wild type plants (A,E), 3-day old wild-type plants germinated on MS without Kyn and transferred to a medium with Kyn and grown for a further 24h (B,G) and 48h (C,F,H). (I,J) *DII-Venus* expression in wild-type plants grown without Kyn (I) and transferred to a medium with Kyn for 4h 30 minutes (J) (Scale bars: 25 µm for longitudinal and 10 µm for cross-sections). Green arrows indicate *DII-Venus* signal appearing in metaxylem. (K,L) Basic fuchsin-stained xylem of 5 day-old wild-type plants (K) and wild-type plants three days after cutting the shoot off (L) (Scale bar: 25 µm). Blue arrows indicate metaxylem and yellow arrows indicate protoxylem.

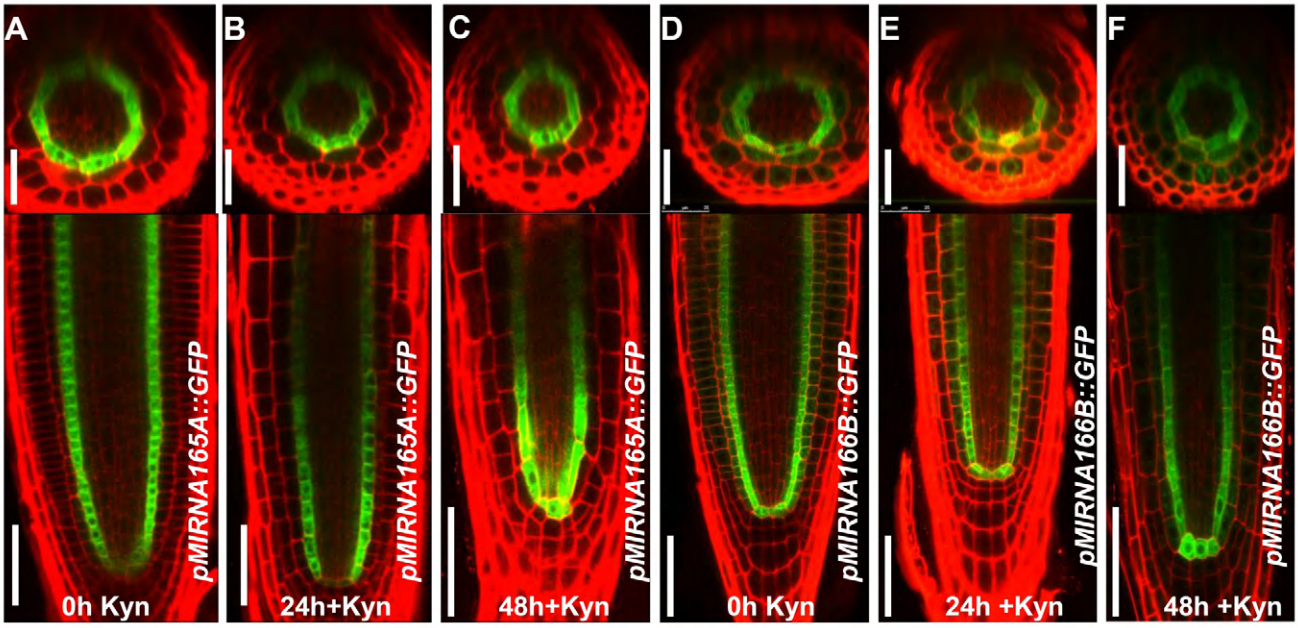

Supplementary Fig. 5. (A-C) *pMIR165A::GFP* in 5-day old wild type plants (A), 3-day old wild-type plants germinated on MS without Kyn and transferred to a medium with Kyn and grown for a further 24h (B) and 48h (C). (D-F) *pMIR166B::GFP* in 5-day old wild type plant (D), 3-day old wild-type plants germinated on MS without Kyn and transferred to a medium with Kyn and grown for a further 24h (E) and 48h (F). (Scale bars: 50 µm for longitudinal and 25 µm for cross sections).

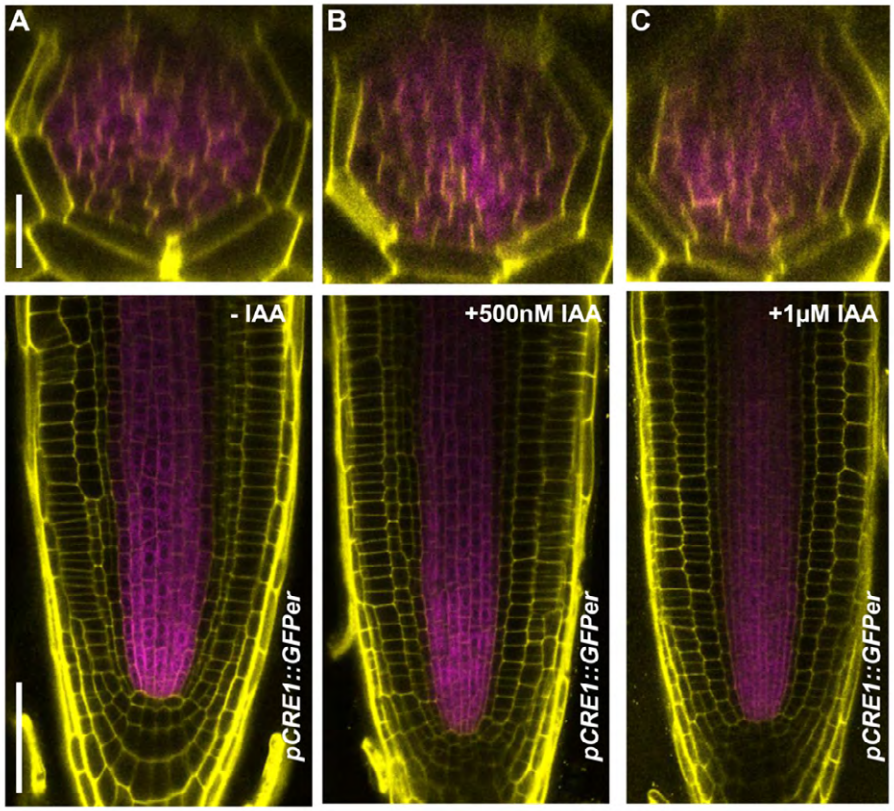

Supplementary Fig. 6. (A-C) *pCRE1::GFPer* expression in wild-type roots grown on a medium without IAA (A), with 500 nM IAA (B) and 1 µM IAA (C) (Scale bar: 50 µm).

Table S1.

SSLP markers used in *trp2-12* mapping process

Marker Name	Sequence (5' to 3')
MN1.5 FP	TTATTATCAAGATCAAAGATTGTATGGTT
MN1.5 RP	CTTGTTTTTATATCTGTTTGGTTTAATTGT
CIW12 FP	AGGTTTTATTGCTTTTCACA
CIW12 RP	CTTTCAAAAGCACATCACA
NGA111 FP	TGTTTTTTAGGACAAATGGCG
NGA111 RP	CTCCAGTTGGAAGCTAAAGGG
NGA1145 FP	GCACATACCCACAACCAGAA
NGA1145 RP	CCTTCACATCCAAAACCCAC
NGA361 FP	ACATATCAATATATTAAAGTAGC
NGA361 RP	AAAGAGATGAGAATTTGGAC
NGA6 FP	ATGGAGAAGCTTACACTGATC
NGA6 RP	TGGATTTCTTCCTCTCTTCAC
NGA172FP	CATCCGAATGCCATTGTTC
NGA172RP	AGCTGCTTCCTTATAGCGTCC
NGA162FP	CTCTGTCACTCTTTTCCTCTGG
NGA162 RP	CATGCAATTTGCATCTGAGG
CIW11 FP	CCCCGAGTTGAGGTATT
CIW11 RP	GAAGAAATTCCTAAAGCATTC
MN4.2 FP	TAAGGTCAGACTATATGTTTACGTTTCATT
MN4.2 RP	GTCATCCTCGTTTAAGTTACGATTG
NGA8 FP	TGGCTTTCGTTTATAAACATCC
NGA8 RP	GAGGGCAAATCTTTATTTCGG

NGA151 FP	CAGTCTAAAAGCGAGAGTATGATG
NGA151 RP	GTTTTGGGAAGTTTTGCTGG
NGA106 FP	TGCCCCATTTTGTTCTTCTC
NGA106 RP	GTTATGGAGTTTCTAGGGCACG
NGA139 FP	GGTTTCGTTTCACTATCCAGG
NGA139 RP	AGAGCTACCAGATCCGATGG
NGA76 FP	AGGCATGGGAGACATTTACG
NGA76 RP	GGAGAAAATGTCACTCTCCACC
MBG8 FP	TGTGCCAGATCTTCGTGTTC
MBG8 RP	GGAAGCTGAGATCTGGACAA
MTH12 FP	GTAAAATTTTCTATTGCA
MTH12 RP	ATGTCCTCCTGTTCTGTCCA
SO191 FP	CTCCACCAATCATGCAAATG
SO191 RP	TGATGTTGATGGAGATGGTCA

Table S2.

CAPS markers used in *trp2-12* mapping

Marker Name	Sequence (5' to 3')	Restriction enzyme
N5-17692527 FP	TCACAGGCAGAGCAAATACG	*NdeI*
N5-17692527 RP	CCAATAAGGACCACCAAAAA	
N5-18568550 FP	TCAATATGATATGCGAGACTTCAGA	*EcorI*
N5-18568550 RP	TCCATGTGCGAATAATAAAAGA	
N5-21038864 FP	GATTCTCATATGCTTCCAGCTGTT	*SspI*
N5-21038864 RP	AGTTGTCATGAGAGCTGATTTGA	
N5-22116697 FP	CCGGGACGGATGTAGTGAT	*HpaI*
N5-22116697 RP	ATTTGATCCTGACCGTTGGA	
N5-23412903 FP	CAGTTTCGGTGCCATGAAC	*EcoRI*
N5-23412903 RP	GAAGGTGCTGGGAGTACAGC	
N5-24832927 FP	TCTTTTTGAGTCATCCATGGTTTT	*XmnI*
N5-24832927 RP	GTTGTTTAACAGGGCCAGCA	

Table S3.

TSB1 gene sequencing primers

Primer Name	Sequence (5' to 3')
TRP2seq1	CCAACCGCTTAGCAAGAAGAGCC
TRP2seq2	GGAAACAAGCGTTGGAGAAATGG
TRP2seq3	CCTGCACTGATGGAGTGTGG

Table S4.

Primers Used in Genotyping

Primer Name	Sequences (5' to 3')
trp2.geno.F	GGAGTCCACTCTGGAACAGC
trp2.geno.R	CGCTTCTTCGTCGGTTATGC
DWLB1	CATACTCATTGCTGATCCATGTAGATTTCC
70560-R1	GCTTTTAATGAGCTTCATGTTGG
70560-F8	CATCAGAGAGACGGTGGTGAAC
24670-F1	GCACGCAAGTGAAGCTCCAAGC
JMLB1	GGCAATCAGCTGTTGCCCGTCTCACTGGTG
iaah.F	ATGGTGGCCATTACCTCGTTAG
iaah.R	CTAATTGGGTAAACCGG
YUC3.F	CTGTCTATGTTATAATCGTCGC
YUC3.R	CTCTCTTGGTAAAACATGAAC
YUC8.F	GAACTGACGCTTCGTCGGGTA
YUC8.R	CATCCTCTCCACGTGGCTTCC
YUC5.F	GGAGATTTCAAAACTAGATTTG
T-DNA	ACCCGACCGGATCGTATCGGT
YUC5.R	CGGACTCTAATCAAAGTCCC
YUC7.F	CATGGAGTGGGCTTATCTCTTTGA
YUC7.R	ACGAAAAACAGAGCACCCTGA
YUC9.F	GAAGGAAATGCCCAATGAGAC
YUC9.R	GCTCGGTAAGCAAAACAAAACTG
SAIl-LB1	GCC TTTTCAGAAATGGATAAATAGCCTTGCTTCC
T-DNA SPM32	TACGAATAAGAGCG CCATTTTAGAGTGA